

A Branch-and-Price Algorithm Enhanced by Decision Diagrams for the Kidney Exchange Problem

Lizeth Carolina Riascos-Álvarez

Department of Mechanical and Industrial Engineering, University of Toronto, Toronto, Ontario M5S 3G8, Canada,
carolina.riascos@mail.utoronto.ca

Merve Bodur

Department of Mechanical and Industrial Engineering, University of Toronto, Toronto, Ontario M5S 3G8, Canada,
bodur@mie.utoronto.ca

Dionne M. Aleman

Department of Mechanical and Industrial Engineering, University of Toronto, Toronto, Ontario M5S 3G8, Canada
Institute of Health Policy, Management and Evaluation, University of Toronto, Toronto, Ontario M5S 3E3, Canada
Techna Institute at University Health Network, Toronto, Ontario M5G 1P5, Canada, aleman@mie.utoronto.ca

Problem definition: Kidney paired donation programs allow patients registered with an incompatible donor to receive a suitable kidney from another donor, as long as the latter’s co-registered patient, if any, also receives a kidney from a different donor. The kidney exchange problem (KEP) aims to find an optimal collection of kidney exchanges taking the form of cycles and chains. **Methodology/results:** We develop the first decomposition method that is able to consider long cycles and long chains for projected large realistic instances. Particularly, we propose a branch-and-price framework in which the pricing problems are solved (for the first time in packing problems in a digraph) through multi-valued decision diagrams. We present a new upper bound on the optimal value of the KEP, obtained via our master problem. Computational experiments show superior performance of our method over the state of the art by optimally solving almost all instances in the PrefLib library for multiple cycle and chain lengths. **Managerial implications:** Our algorithm also allows the prioritization of the solution composition, e.g., chains over cycles or vice versa, and we conclude, similar to previous findings, that chains benefit the overall matching efficiency and highly sensitized patients.

Key words: Kidney exchange; integer programming; branch and price; multi-valued decision diagrams

1. Introduction

The preferred treatment for kidney failure is transplantation, and demand for deceased-donor kidneys usually outnumbers supply (CIHI 2019). An alternative, often desirable, is living-donor transplantation. A living donor is typically a close relative, partner or friend who is willing to

donate one of their kidneys to grant a life-saving chance to a beloved one. However, biological incompatibilities, such as blood type or antibodies related discrepancies, between the patient in need of a kidney and the potential donor may exist. It is in these cases where Kidney Paired Donation Programs (KPDPs), present in multiple countries, have played a life-saving role in kidney transplantation systems. A KPDP is a centralized registry operated at a local or national level, where each patient registers voluntarily along with his or her incompatible (suboptimal) donor (*paired donor*) as a pair. Patients in these patient-donor pairs (PDPs) are willing to exchange their paired donors under the promise that they will receive a suitable kidney from a different donor. To accomplish this goal, two types of exchanges are allowed: cyclic and chain-like exchanges.

Figure 1a illustrates a pool of six patient-donor pairs $(p_1, d_1), (p_2, d_2), \dots, (p_6, d_6)$ arranged in two cycles. In the cyclic exchange on the left, donor d_2 donates to patient p_1 and donor d_1 donates to patient p_2 , thereby forming a *cycle*. On the right, a cycle involving four PDPs is depicted, where donor d_4 donates a kidney to patient p_3 and patient p_4 receives a kidney from donor d_6 , after sequential donations. Due to pair drop-outs, aggravated health condition of a pair member, or last-minute detected incompatibilities, the patient in the first pair may never receive a kidney back if the donor in any subsequent pair in the cycle fails to donate. To avoid such a risk, cycles of kidney transplants are performed simultaneously in practice, imposing limitations on K , the maximum size of a cycle, where $K \in \mathbb{Z}_+$. In the literature, a k -way cycle refers to a cycle involving k transplants, with $k \leq K$. Although in some countries such as the United States, it is common to find $K = 3$ (Flechner et al. 2018), other countries have reported longer cycles (Malik and Cole 2014, Cantwell et al. 2015), up to $K = 6$ in Canada (Canadian Blood Services 2019).

In the presence of singleton donors, chains become an exchange alternative. Some singleton donors are *altruistic donors* because they are willing to donate one of their kidneys without having a paired patient; such donors are represented as vertices with outgoing arcs to any feasible patient-donor pair vertex, and no incoming arcs. A *chain* is a path that starts with a singleton donor donating to a patient in a PDP, after which all remaining patients receive a kidney from a paired

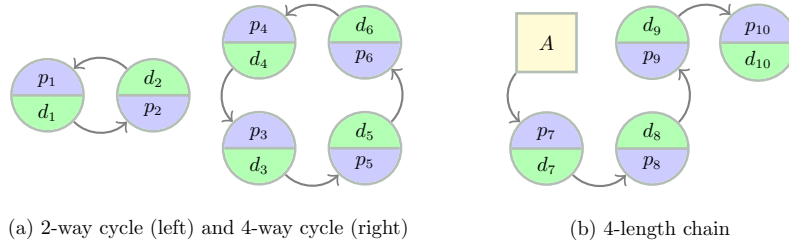


Figure 1 Examples of exchanges. PDPs are represented by circle nodes, while the NDD is square.

donor (Figure 1b). The donor in the last pair of a chain can either donate to a patient on the transplant waitlist or become a *bridge donor* (a single donor in a future chain). In general, chain-initiating donors such as altruistic, bridge, or even deceased donors (Wall et al. 2018), are referred to as *non-directed donors* (NDDs). Unlike cycles, no paired donor in a chain risks not receiving a kidney for their intended recipient, making it possible to relax the simultaneity constraint. Since simultaneous surgeries (e.g., six surgeries for a three-way cycle) may bring capacity and logistics challenges, a simultaneity requirement poses stronger restrictions on the maximum cycle length than on the maximum chain length (Dickerson et al. 2012, Biró et al. 2021). To the best of our knowledge, chains are unbounded in the nationwide KPDP in the United States (Dickerson et al. 2012). These very long chains can be carried out in practice through the use of bridge donors that connect multiple segments of the same chain. In most European countries, both cycles and chains are carried out simultaneously (Biró et al. 2021), which results in shorter algorithmic chains compared to the United States, but still considered long (up to six transplants) in some European countries, e.g., Czech Republic and Italy (Biró et al. 2021). The Canadian KPDP allows long chains with up to six transplants that are not necessarily performed simultaneously (Canadian Blood Services 2019). Thus, very often, the maximum chain length $L \in \mathbb{Z}_+$ is as big or bigger than K ($L \geq K$).

As some transplants may be more suitable or urgent from medical and logistical points of view, a score may be given to every potential transplant. A common objective in kidney exchange, although not the only one, is to match donors (paired and singleton) to patients such that the sum of the transplants' score is maximized (Abraham et al. 2007, Roth et al. 2007). The matching must satisfy

that every PDP belongs to at most one cycle or chain and every NDD to at most one chain. Finding a matching of maximum score in this context is known as the *kidney exchange problem* (KEP).

Depending on the country’s population and matching frequency, the average instance size may vary. For instance, [Dickerson et al. \(2016\)](#) used real match runs from the UNOS program which have on average <250 PDPs and a low number of altruists, which may be explained by the semi-weekly matching frequency. In Canada, matching frequency is every four months, with an average instance size around 150 PDPs and ≤ 12 NDDs with maximum cycles and chain lengths of 6 ([Canadian Blood Services 2019](#)). The literature has frequently tested matching algorithms not only with respect to the current size of instances, but with respect to expected instance size increases in the future, e.g., 500 ([Glorie et al. 2014](#)), 700 ([Dickerson et al. 2016](#)), and 10,000 PDPs ([Abraham et al. 2007](#)). Additionally, problem sizes increase with collaborations among multiple KPDPs sharing participant pools with either other co-national programs or within organized large-scale international exchanges ([Ashlagi and Roth 2021](#), [Klimentova et al. 2021](#), [Rees et al. 2017](#)), e.g., a recent collaborative pilot program between the Italian National Transplant Center and the Alliance for Paired Kidney Donation from the United States ([Trapiantti 2022](#)). These collaborations bring new operational and algorithmic challenges due to possibly larger exchange pools that may benefit from longer cycles and chains.

Therefore, motivated by practical settings for which $K \geq 4$ along with long chains ([Malik and Cole 2014](#), [Ashlagi and Roth 2021](#)), previous studies showing the value of long chains ([Ashlagi et al. 2012](#), [Dickerson et al. 2012](#), [Ding et al. 2018](#)), the increasing number of participants in KPDPs, and space for improvement in state-of-the-art approaches, we develop a new solution technique for the KEP. Particularly, we make the following contributions:

1. We devise a B&P algorithm that incorporates cycles and long chains and solve the pricing problems via multi-valued decision diagrams (MDDs). To the best of our knowledge, this is the first study using MDDs in cycle and path packing problems in a digraph, and one of the two works in the B&P literature ([Raghunathan et al. 2018](#)). Our B&P

-
- Is the first *correct*¹ B&P algorithm for the cycles-and-chains variant (Omer et al. 2022).
 - Provides an exact optimal solution.
 - Can scale to instances sizes not previously possible.
 - Allows the prioritization of cycles over chains and vice-versa, properties that are desirable in practice even when the instances are small enough for other algorithms to solve to optimality.
2. We present an effective three-phase solution method for the pricing problems, shifting between MDDs and linear (worst-case integer) programs.
 3. We present the first use of Lagrangian relaxation in this context. Additionally, we show for the first time that the dual of our Lagrangian relaxation formulation is equivalent to the disaggregated cycle formulation (Klimentova et al. 2014). This observation allowed us to propose the only other known upper bound on the optimal value of the KEP, which is tighter than the previously proposed upper bound (Abraham et al. 2007), while recent works provided no upper bound for instances that timed out (Lam and Mak-Hau 2020).
 4. We demonstrate computational improvement over state-of-the-art methods on publicly available instances.
 5. Given that multiple optima can exist in KEP (Klimentova et al. 2021), and that some of them may be preferred for logistical or fairness reasons, our algorithm allows the prioritization of chains or cycles in a single run. Additionally, we perform an experimental analysis showing the impact of the chain/cycle composition of multiple solutions.
 6. We empirically demonstrate the benefits of chains for different graph densities and sizes, taking into account the presence of highly sensitized patients. Our results are in agreement with previous studies (Ashlagi et al. 2012, Dickerson et al. 2012, Ding et al. 2018).

Additionally, we note that while B&P implementations are always bespoke frameworks for the particular application at hand, our framework could generally be used to detect large cycles and/or

¹ The first B&P to ever address the cycles-and-chains variant was published in M&SOM (Glorie et al. 2014), but was later shown to be incorrect (Plaut et al. 2016a).

chains in networks, which has applications in prize-collecting traveling salesman problems and in longest-path problems on non-directed acyclic graphs. Moreover, the number of the MDDs for cycles provides a feasible solution to the feedback vertex set problem. Additionally, our framework could be used in applications for sequencing problems that can be formulated as MDDs, e.g., multicommodity pick-up-and delivery TSP (Castro et al. 2020).

The rest of the paper is organized as follows. In Section 2, we review the relevant literature. In Section 3, we present a formal definition of the KEP. In Section 4, we detail our B&P algorithm, including the reformulation of pricing problems via MDDs. In Section 5, we present our general solution approach. In Section 6, we show experimental results comparing our algorithm with the state of the art. Lastly, we draw some conclusions and point to future work in Section 7.

2. Literature Review

A very-well studied variant of the KEP is the cycle-only version, i.e., a problem instance in which either there are no NDDs or if present, chains are “turned” into cycles by adding an arc from every PDP to NDDs. As a result, the maximum length is the same for both cycles and chains. Different methods, mostly mixed integer programming (MIP) but also heuristics (see, e.g., the cycle-only approach by Delorme et al. (2022)), have been used to model this variant of the KEP in the literature. While heuristics can be fast and are often worth a trade-off in optimality for speed, in the specific example of KEP, being able to match even just one more patient per matching can be life-changing for that one person. In countries where matchings are infrequent (e.g., matchings are only done every four months in Canada), having to wait just one more round of matching to receive a kidney could be very damaging to the patient’s deteriorating health and quality of life. Thus, from both a practical and a philosophical point of view, if we can tractably solve large KEP instances to optimality, there is benefit to choosing an optimal approach over a heuristic, and therefore we focus on optimal MIP approaches in the literature.

Abraham et al. (2007) and Roth et al. (2007) proposed two widely known MIP formulations: the *cycle formulation*, which has an exponential number of decision variables, and the *edge formulation*,

which has an exponential number of constraints. [Constantino et al. \(2013\)](#) showed that the edge formulation scales substantially worse than the cycle formulation, reaching more than three million constraints in instances with only 50 PDPs, while the cycle formulation leads to memory issues when $K \geq 4$ in medium and high density instances with 100 PDPs or more.

[Constantino et al. \(2013\)](#) proposed the first two MIP formulations where the number of constraints and variables are polynomial in the size of the input, referred to as *compact formulations*. It was shown that their *extended edge formulation* outperforms their *assignment edge formulation*. Although the cycle formulation is theoretically stronger than both, the extended edge formulation is able to scale in instances where the cycle formulation requires more than three million variables.

B&P ([Barnhart et al. 1998](#)) is commonly used to overcome the exponential number of variables of the cycle formulation, yielding the most successful solution methods for the KEP to date ([Abraham et al. 2007](#), [Klimentova et al. 2014](#), [Dickerson et al. 2016, 2019](#)). For cycle-only KEP, the state of the art is the B&P-and-cut developed by [Lam and Mak-Hau \(2020\)](#), where the cycle formulation is used as a master problem, and few cuts were added to the master problem in most runs on problem instances from the PrefLib library ([Mattei and Walsh 2013](#)). Most instances with 2048 PDPs and $K = 3$ reported total run-time of 2s and for the majority of instances with up to 1024 PDPs, $< 1s$. For $K = 4$ only instances with up to 1024 PDPs could be solved, taking up to 22min.

In the general version of the KEP, chains are allowed, and usually $L \geq K$ or unbounded. [Anderson et al. \(2015\)](#) proposed two formulations for unbounded chains: recursion and a prize-collecting traveling salesman problem (PC-TSP) variation. Instances with up to 1179 PDPs and 62 NDDs were tested with $K = 3$. The recursive formulation outperformed the PC-TSP formulation on a large historical dataset, although, in “difficult” instances, the PC-TSP formulation was more successful. This formulation can be modified to include bounds on the length of chains. However, [Plaut et al. \(2016a\)](#) showed that the PC-TSP is effective when unbounded chains and $K = 3$ are considered, otherwise, B&P-based algorithms outperform it.

[Mak-Hau \(2015\)](#) introduced two formulations (EE-MTZ and SPLIT-MTZ), inspired by [Abraham et al. \(2007\)](#), [Constantino et al. \(2013\)](#) and the well-known Miller-Tucker-Zemlin constraints. The

largest instance presented includes 250 PDPs and 6 NDDs with arc density of 5%. Overall, EE-MTZ optimally solves more instances than SPLIT-MTZ.

[Dickerson et al. \(2016\)](#) proposed three formulations: a compact formulation for the cycle-only version, PIEF, a compact variation of PIEF allowing long chains, HPIEF, and an exponential-sized formulation also allowing long chains, PICEF. The first two formulations are adapted from the extended edge formulation and the last one is inspired by both the extended edge formulation and the cycle formulation. Instances from real match runs and from a realistic simulator were used to test seven algorithms ([Abraham et al. 2007](#), [Klimentova et al. 2014](#), [Anderson et al. 2015](#), [Glorie et al. 2014](#), [Plaut et al. 2016b](#), [Dickerson et al. 2016](#)), with $K = 3$ and a time limit of 1h. On real match runs from the United Kingdom, the algorithm by [Klimentova et al. \(2014\)](#) outperformed the others when no NDDs were included. However, for larger (simulated) instances with up to 700 PDPs and 171 NDDs, HPIEF and PICEF were the most effective solution methods. A direct search approach for the pricing problem ([Abraham et al. 2007](#)) enumerates all cycles in the worst case, which is exponential when also considering chains (the search for chains is $\mathcal{O}(|N||P|^L)$ and the search for cycles is $\mathcal{O}(|P|^K)$). Unlike the dynamic programming algorithms in [Glorie et al. \(2014\)](#) and [Plaut et al. \(2016b\)](#), which were shown incorrect for the cycles-and-chains variant ([Plaut et al. 2016a](#)), our solution to the pricing problems occurs in acyclic graphs (our MDDs), which are based on our cycle and chain copies of the input graph. By construction of the copies, there is no positive cycle or chain in the compatibility graph if none is found in the corresponding copy. Thus, our recursive function simply becomes the computation of the longest path in an acyclic network, which can be performed efficiently.

More recently, [McElfresh et al. \(2019\)](#) proposed the position-indexed traveling-salesman problem formulation (PI-TSP) as part of a robust optimization model in which cycles are handled as in the cycle formulation, and chains are expressed by combining the indexing scheme presented in PICEF and ideas from the PC-TSP formulation. Experimentally, robust solutions were compared to deterministic solutions obtained by PICEF.

Other variations of the KEP include finding robust solutions (Dickerson 2014, McElfresh et al. 2019, Carvalho et al. 2020), solutions that maximize the expected number of transplants (Kliimentova et al. 2016, Alvelos et al. 2019) and a matching that optimizes the best outcome over time (Awasthi and Sandholm 2009, Monteiro et al. 2021). Most of these approaches determine a matching that maximizes the number of transplants without distinguishing among several optima. However, real-world applications often require multiple criteria to break ties (Glorie et al. 2014, Biró et al. 2019). Tie-breaking criteria has been studied as an ordered list of objectives that are solved sequentially by adding rationality constraints (Glorie et al. 2014). While our main goal remains to maximize the number of transplants, we consider the prioritization of an exchange type (cycles or chains) as a second objective. We achieve this goal by strategically including columns in our column generation algorithm, allowing us to optimize both objectives in a single run.

3. Problem Description

Given a set of PDPs \mathcal{P} , a set of NDDs \mathcal{N} , and positive integers K and L , the KEP can be defined in a digraph $\mathcal{D} = (\mathcal{V}, \mathcal{A})$. A vertex $v \in \mathcal{V}$ is defined for each PDP and NDD, i.e., $\mathcal{V} = \mathcal{P} \cup \mathcal{N}$. For $v_i, v_j \in \mathcal{V}$, there exists an arc $(v_i, v_j) \in \mathcal{A}$ if the donor in vertex v_i is compatible with the patient in vertex v_j , e.g., see Figure 1, which illustrates possible chain and cycle solutions. Note that, $\mathcal{A} \subseteq \{(v_i, v_j) \mid v_i \in \mathcal{V}, v_j \in \mathcal{P}\}$, that is, there are no incoming arcs to NDDs, neither from PDPs nor from the other NDDs. Each arc (v_i, v_j) is assigned a score w_{ij} representing the suitability/priority of that transplant, where suitability refers to the quality of the match from a medical perspective. With these weights, priorities for transplants can represent varying priority rules, e.g., preference to match highly sensitized patients, patients that have been on the waitlist longest, etc.

Chains and cycles correspond to simple paths and cycles of \mathcal{D} , respectively, formally defined as follows:

DEFINITION 1. A chain $p = (v_1, \dots, v_\ell)$ is feasible if and only if: (1) $(v_i, v_{i+1}) \in \mathcal{A} \ \forall i = 1, \dots, \ell - 1$, (2) $v_1 \in \mathcal{N}$ and $v_i \in \mathcal{P} \ \forall i = 2, \dots, \ell$, and (3) $\ell \leq L + 1$. Note that for a chain to include L transplants, $L + 1$ vertices are required.

DEFINITION 2. A cycle $c = (v_1, \dots, v_k, v_1)$ is feasible if and only if: (1) $(v_i, v_{i+1}) \in \mathcal{A} \forall i = 1, \dots, k-1$ and $(v_k, v_1) \in \mathcal{A}$, (2) $v_i \in \mathcal{P} \forall i = 1, \dots, k$, and (3) $k \leq K$.

A feasible solution to the KEP is a matching of donors to patients. To formally introduce this definition, consider \mathcal{C}_K and \mathcal{C}_L as the set of all feasible cycles and chains in \mathcal{D} , respectively. Throughout the paper, notation $\mathcal{V}(\cdot)$ and $\mathcal{A}(\cdot)$ will denote the set of vertices and arcs present in the argument (\cdot) , respectively. For instance, $\mathcal{V}(c)$ corresponds to the set of vertices in cycle c .

DEFINITION 3. $M(K, L) \subseteq \mathcal{C}_K \cup \mathcal{C}_L$ is a feasible matching of donors to patients if $\mathcal{V}(m_1) \cap \mathcal{V}(m_2) = \emptyset$ for all $m_1, m_2 \in M(K, L)$ such that $m_1 \neq m_2$.

That is, a matching in the KEP corresponds to a collection of feasible chains and cycles where every patient/donor participates in at most one transplant and type of exchange. Thus, the objective of the KEP is to find a matching, whose set of arcs $\mathcal{A}(M(K, L))$ maximizes the total transplant score, i.e., $\sum_{(i,j) \in \mathcal{A}(M(K,L))} w_{ij}$.

4. B&P Algorithm

Our approach to KEP is, to the best of our knowledge, the only B&P for KEP valid for long, yet bounded chains. For completeness, we first discuss the general motivation behind B&P. We then detail our B&P implementation. Particularly, we focus on solving the pricing problems via multi-valued decision diagrams, a solution method novel to cycle and path packing problems in digraphs, and only used before in a transportation scheduling problem ([Raghunathan et al. 2018](#)), to the best of our knowledge.

4.1. Background

Instead of considering the full set of variables in a linear program, *column generation* works with a small subset of variables (*columns*), forming the well-known *restricted master problem* (RMP). If by duality theory a column is missing in the RMP, a cycle or chain with positive-reduced cost must be found and added to the RMP to improve its current objective value. To find such a column(s) one can solve tailored *pricing problems*, which return either a “positive-price” cycle (chain) or a certificate that none exists. RMP and pricing problems are solved iteratively, typically, until

strong duality conditions are satisfied. Since the solution of the RMP may not be integer, column generation is embedded into a branch-and-bound algorithm to obtain an optimal solution, yielding a B&P algorithm.

4.2. Restricted master problem

We use the linear programming relaxation of the disaggregated cycle formulation (**IDCF**), proposed in [Klimentova et al. \(2014\)](#) as our RMP, which starts with zero columns. In this formulation, the input digraph $\mathcal{D} = (\mathcal{V}, \mathcal{A})$ is disaggregated into copies of two types: cycles and chains. The goal is to obtain a feasible cycle and a feasible chain from each of such copies, starting with a unique vertex. This unique vertex in a chain copy is an NDD and its copy of the graph consists of the chains triggered by it. The unique vertex is called a *feedback vertex* for cycle copies, and the graph copy consists of all cycles to which this feedback vertex belongs. We define $\mathcal{V}^* \subseteq \mathcal{V}$ as the set of feedback vertices in the digraph. As an example, consider the digraph shown in [Figure 2a](#). If we set $\mathcal{V}^* = \{4, 5\}$, then two cycle copies ([Figures 2b](#) and [2c](#)) include all cycles of the input digraph. More details on the use of feedback vertices follow in [Section 4.3.2](#).

The number of cycle copies is governed by an upper bound $|\mathcal{V}^*|$ on the number of cycles in a feasible KEP solution, and the number of chain copies is given by the number of NDDs. Shortly, our goal will become to find those graph copies (for cycles and chains) and their associated MDD.

Thus, for every cycle copy indexed by $\hat{I} = \{1, \dots, |\mathcal{V}^*|\}$ and for every chain copy indexed by $\bar{I} = \{1, \dots, |\mathcal{N}|\}$, there exists a cycle (chain) decision variable z_c^i (z_p^i) associated to the i th graph copy. Letting $\hat{\mathcal{C}}_K^i$ be the set of cycles in the i th graph copy limited to cycles with up to K exchanges, and $\bar{\mathcal{C}}_L^i$ defined similarly for chains, the disaggregated cycle formulation of the RMP is

$$\max \sum_{i \in \hat{I}} \sum_{c \in \hat{\mathcal{C}}_K^i} w_c z_c^i + \sum_{i \in \bar{I}} \sum_{p \in \bar{\mathcal{C}}_L^i} w_p z_p^i \quad (\text{IDCF})$$

$$\sum_{i \in \hat{I}} \sum_{c \in \hat{\mathcal{C}}_K^i : v \in \mathcal{V}(c)} z_c^i + \sum_{i \in \bar{I}} \sum_{p \in \bar{\mathcal{C}}_L^i : v \in \mathcal{V}(p)} z_p^i \leq 1 \quad v \in \mathcal{V} \quad (1a)$$

$$z_c^i \geq 0 \quad i \in \hat{I}, c \in \hat{\mathcal{C}}_K^i \quad (1b)$$

$$z_p^i \geq 0 \quad i \in \bar{I}, p \in \bar{\mathcal{C}}_L^i \quad (1c)$$

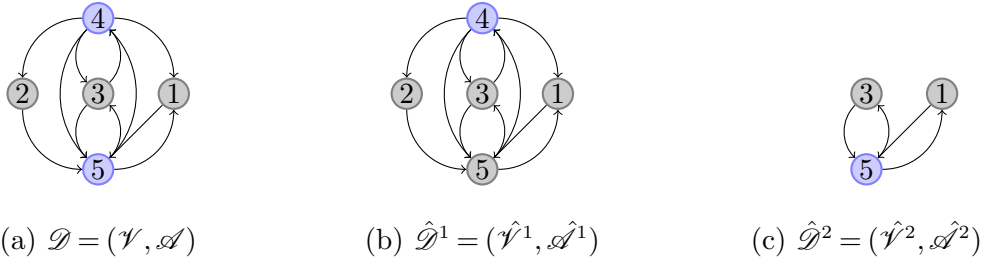


Figure 2 Graph disaggregation. Blue vertices correspond to feedback vertices. (a) Complete digraph; (b) vertex 4 is the feedback vertex; (c) vertex 5 is the feedback vertex

The objective value maximizes the weighted sum of feasible cycles and chains, whereas Constraints (1a) restrict every vertex to be selected in at most one cycle or chain, and thus, in at most one graph copy.

4.3. MDDs for the Pricing Problem

The pricing problem in this context corresponds to finding a feasible cycle or a feasible chain with positive reduced cost. If the reduced cost of a cycle or chain is positive (thus, a positive-price column), then such column should be added to the RMP. The reduced cost of a cycle and chain can be defined, for example, by the objective function of MIP formulations (CC) and (CH), respectively, (see Online Appendix A). Solution methods to the pricing problem in the literature for the cycle-only version include heuristics (Abraham et al. 2007), MIP (Roth et al. 2007), or a combination of exact and heuristic algorithms (Klimentova et al. 2014, Lam and Mak-Hau 2020). Also, Glorie et al. (2014) and Plaut et al. (2016b) tackled this version by using a modified Bellman-Ford algorithm in a reduced graph, for the cycle-only version (Plaut et al. 2016a). Pricing algorithms including long chains have been less studied. Dickerson et al. (2019) studied heuristics for generating positive-price short cycles and arbitrarily large chains when their expected utility is maximized. Our goal is to solve the pricing problems efficiently for both long cycles and long chains by means of MDDs.

4.3.1. Decision Diagrams A decision diagram is a graphical data structure, used in optimization to represent the solution set of a given problem. Particularly, a decision diagram is a rooted, directed and acyclic layered graph, where (if *exact*), every path from the root node \mathbf{r} to a

terminal node \mathbf{t} has a one-to-one correspondence with a solution in the feasible space of the optimization problem. If the objective function is arc separable, then a shortest-path-style algorithm can be used to find the optimal objective value. When the domain of decision variables represented in the diagram includes three or more values, the decision diagram is an MDD. [Cire and van Hoeve \(2013\)](#) proposed solving sequencing problems using MDDs and showed primary applications in scheduling and routing, (see also [Kinable et al. \(2017\)](#), [Castro et al. \(2020\)](#)). The only work we are aware of, in which MDDs are used to solve pricing problems, is by [Raghunathan et al. \(2018\)](#). They tackle a last-mile transportation problem in which passengers reach their final destination by using a last-mile service system linked to the terminal station of a mass transit system. A path in these MDDs represents a partition of passengers sharing trip characteristics.

4.3.2. Construction of MDDs for the KEP Decision diagrams can be constructed by finding the *state transition graph* of a dynamic programming (DP) formulation and reducing it afterwards (see [Cire and van Hoeve \(2013\)](#), [Hooker \(2013\)](#) for more details). We model the pricing problems by formulating two DP models; for cycles and chains. Particularly, a DP model is formulated for each cycle copy $i \in \hat{I}$, and for each chain copy $i \in \bar{I}$. A *state* in these models represents the vertices $v \in \mathcal{V}$ visited at previous *stages*, where a stage corresponds to the position of a vertex in a cycle or chain. *Controls* $\hat{h}^{|K|}$ and $\bar{h}^{|L|}$ take the index value of a vertex $v \in \mathcal{P}$ and vertex $v \in \mathcal{V}$, indicating that it is assigned to a cycle or chain, respectively, in the position given by the control index, i.e., in position $k \leq K$ of a cycle or position $\ell \leq L$ of a chain. Since the domain of \hat{h} and \bar{h} variables contains three or more values, the resulting diagram is an MDD.

While it is easy to derive the number of MDDs for chains (one for every NDD), that is not the case for cycles. As a result, we start by considering \mathcal{V}^* as a “ K -limited” *feedback vertex set* (FVS), i.e., a set of vertices whose removal from the graph removes all feasible cycles. We refer to vertices in this set as *feedback vertices*. Note that when K is sufficiently large, a K -limited FVS corresponds to an FVS of \mathcal{D} . The goal is then to find a “small” cardinality K -limited FVS to build as few MDDs for cycles as possible; one for each vertex in \mathcal{V}^* . Since finding a minimum FVS and a smallest set covering are NP-hard problems ([Karp 1972](#)), we introduce a heuristics as an alternative.

Algorithm 1: K -limited FVS heuristics

Result: Feedback vertex set $\mathcal{V}^* \subseteq \mathcal{V}$ and decision diagrams $\hat{\mathcal{G}}^i = (\hat{\mathcal{N}}^i, \hat{\mathcal{A}}^i) \forall i \in \hat{I}$

Input: Digraph $\mathcal{D} = (\mathcal{V}, \mathcal{A})$, vertex ordering \mathcal{S} , maximum length K

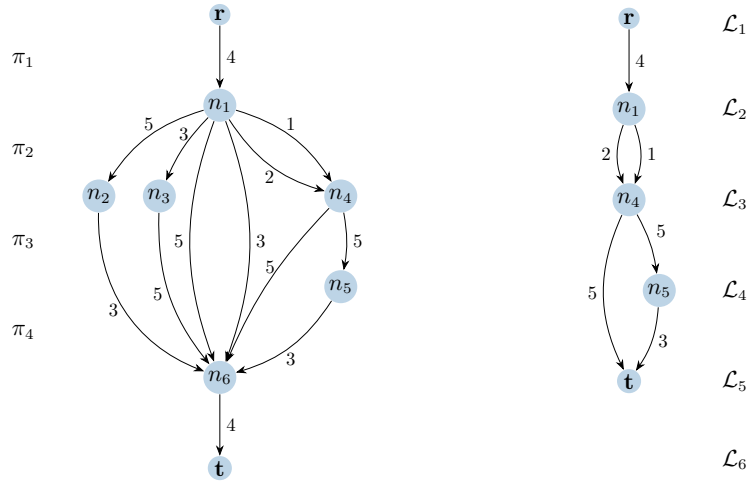
```

1  $\mathcal{V}^* = \emptyset, \hat{I} = \emptyset, i = 0$ 
2 while  $|\mathcal{S}| \geq 1$  do
3    $v^* \leftarrow s_1 \in \mathcal{S}$ 
4    $V \leftarrow \mathcal{V} \setminus \mathcal{V}^*$ 
5    $A \leftarrow \{(u, v) \in \mathcal{A} : u, v \in V\}$ 
6    $\hat{\mathcal{G}} = (\hat{\mathcal{N}}, \hat{\mathcal{A}}) \leftarrow \text{BuildMDD}(v^*, D = (V, A))$ 
7   if  $\hat{\mathcal{A}} \neq \emptyset$  then
8      $i \leftarrow i + 1, \hat{I} \leftarrow \hat{I} \cup \{i\}$ 
9      $\hat{\mathcal{G}}^i = (\hat{\mathcal{N}}^i, \hat{\mathcal{A}}^i) \leftarrow \hat{\mathcal{G}} = (\hat{\mathcal{N}}, \hat{\mathcal{A}})$ 
10     $\mathcal{V}^* \leftarrow \mathcal{V}^* \cup \{v^*\}$ 
11     $\mathcal{S} \leftarrow \mathcal{S} \setminus \{v^*\}$ 

```

Algorithm 1 provides a mechanism to obtain a K -limited FVS $\mathcal{V}^* = \{v_1^*, \dots, v_{|\mathcal{V}^*|}^*\} \subseteq \mathcal{D}$ and cycle MDDs $\hat{\mathcal{G}}^i = (\hat{\mathcal{N}}^i, \hat{\mathcal{A}}^i)$, indexed by $\hat{I} = \{1, \dots, |\mathcal{V}^*|\}$. The procedure takes as input a digraph \mathcal{D} and an ordered set \mathcal{S} of PDPs in \mathcal{D} , sorted according to a vertex-ordering rule (e.g., maximum in-degree of a vertex). While there is at least one element in \mathcal{S} , the first vertex in that set denoted by s_1 , is selected as the next potential feedback vertex v^* . Subsequently, the function `BuildMDD` creates a transition graph starting at v^* and reduces it to an MDD. If the set of arcs $\hat{\mathcal{A}}$ is not empty, then a new cycle MDD is created. Vertex v^* is removed from \mathcal{S} afterwards, and a new iteration starts.

The MDD $\hat{\mathcal{G}}^i = (\hat{\mathcal{N}}^i, \hat{\mathcal{A}}^i)$ for the i th cycle copy of \mathcal{D} has its node set $\hat{\mathcal{N}}^i$ partitioned into K layers, $\mathcal{L}_1, \dots, \mathcal{L}_K$, corresponding to the decision of which PDP belongs to the k th position in a cycle, denoted by π_k , plus two terminal layers \mathcal{L}_{K+1} and \mathcal{L}_{K+2} representing the completion of a feasible cycle. Layers $\mathcal{L}_1, \mathcal{L}_2, \mathcal{L}_{K+1}$ and \mathcal{L}_{K+2} have a single node each. Every arc $a \in \hat{\mathcal{A}}^i$ has an associated label $val(a) \in \hat{\mathcal{V}}^i$ such that $\pi_k = val(a)$ corresponds to assigning vertex $val(a)$ to the k th position of a cycle. Since a cycle in the i th cycle copy starts with the i th feedback vertex, then $\pi_1 = v_i^*$. Thus, an arc-specified path (a_1, \dots, a_k) from nodes \mathbf{r} to \mathbf{t} defines the PDP sequence $(\pi_1, \dots, \pi_k) = (val(a_1), \dots, val(a_k))$, equivalent to a feasible cycle in \mathcal{D} . On the other hand, the set of nodes $\bar{\mathcal{N}}^i$ for the i th MDD of a chain copy, $\bar{\mathcal{G}}^i = (\bar{\mathcal{N}}^i, \bar{\mathcal{A}}^i)$, is partitioned into $L + 2$ layers, with



(a) Vertex 4 is a PDP. Exact decision diagram, $K = 4$
 (b) Vertex 4 is an NDD. Restricted decision diagram, $L = 3$

Figure 3 MDDs for the example of Figure 2b.

a single node in the first and last layer, representing the start and end of a chain, respectively. Recall that for a chain to involve L transplants, $L + 1$ vertices $v \in \mathcal{V}$ are required. Likewise, an arc $a \in \bar{\mathcal{A}}^i$ has a label $\pi_\ell = \text{val}(a)$ indicating the vertex $v \in \bar{\mathcal{V}}^i$ at the ℓ th position in a chain, noticing that $\pi_1 = u_i$. A path starting at the root node \mathbf{r} and ending at a node on the third layer or higher represents a feasible chain, since its length is at least one.

Figure 3a depicts all possible sequences of PDPs $\pi_1, \pi_2, \dots, \pi_k$ encoding feasible cycles on the graph copy of Figure 2b. A value π_k placed on an arc corresponds to the k th vertex $v \in \mathcal{P}$ in a cycle covered by vertex 4. For instance, the path $(\mathbf{r}, n_1, n_3, n_6, \mathbf{t})$ in Figure 3a encodes the cycle $c = \{4, 3, 5, 4\}$ in Figure 2b.

Since exact MDDs can grow exponentially large, it might be necessary to limit their size, turning them into *restricted* decision diagrams. A decision diagram is called restricted if the set of solutions corresponding to its \mathbf{r} - \mathbf{t} paths is a subset of the entire feasible set of solutions. Figure 3b shows a restricted MDD as if vertex 4 in Figure 2b were an NDD. In this example, the MDD is restricted to have chains including only two out of the four vertices receiving an arc from vertex 4; namely, vertices 1 and 2.

4.3.3. Finding a positive-price column Since the reduced cost of a cycle (or chain) in the i th MDD, \hat{r}_c^i (or \bar{r}_p^i), is arc separable (Glorie et al. 2014), we proceed to show how to find positive-price columns via MDDs:

Let $\delta_-^i(n_s) \subset \hat{\mathcal{A}}^i$ be the set of incoming arcs to a node n_s in $\hat{\mathcal{N}}^i$ and $\ell(a)$ the layer index of the source node of arc a , e.g., in Figure 3a $\delta_-^i(n_4) = \{(n_1, n_4)^1, (n_1, n_4)^2\}$ and $\ell((n_1, n_4)^1) = 2$, where the superscripts distinguish the two arcs coming into n_4 , one with $\pi_2 = 1$ and the other with $\pi_2 = 2$. Moreover, let λ be the dual variables of Constraints 1a. We define the recursive function values of an arc $a = (n_s, n_{s'})$ for the i th MDD for cycles and chains, $\hat{\eta}^i(a)$ and $\bar{\eta}^i(a)$, respectively, as the maximum reduced cost of all paths ending at a :

$$\hat{\eta}^i(a) = \bar{\eta}^i(a) = \begin{cases} 0 & n_s = \mathbf{r} & (2a) \\ \max_{a' \in \delta_-^i(n_s)} \{ \hat{\eta}^i(a') + w_{val(a'), val(a)} - \lambda_{val(a')} \} & \text{otherwise} & (2b) \end{cases}$$

The recursive function (2) is valid by Bellman's principle of optimality since the reduced cost of a cycle or chain is arc separable and the portion taken by every arc only depends on the previous PDP or NDD in the sequence. Thus, the maximum reduced cost of a cycle and chain, $\hat{\eta}^i$ and $\bar{\eta}^i$, respectively, is given by

$$\hat{\eta}^i = \max \{ 0, \hat{\eta}^i((n, \mathbf{t})) \} \quad i \in \hat{I} \quad (3a)$$

$$\bar{\eta}^i = \max \left\{ 0, \max_{a \in \bar{\mathcal{A}}^i: \ell(a) \geq 3} \bar{\eta}^i(a) - \lambda_{val(a)} \right\} \quad i \in \bar{I} \quad (3b)$$

where for a terminal node \mathbf{t} in a cycle, n is the only node on the $K + 1$ layer with an arc pointing to \mathbf{t} (e.g., node n_6 in Figure 3a), providing a terminal condition for the recursion for cycles.

Recursion (3a) computes the maximum reduced cost of a cycle at the terminal node \mathbf{t} , since all paths need to reach \mathbf{t} to close it up. For chains, on the other hand, any portion of a path in $\bar{\mathcal{G}}^i$ is a feasible path, for which the longest path can be found at any layer of the MDD where the length of a chain (in terms of arcs in $\bar{\mathcal{A}}^i$) is at least one. The term subtracted in Equation (3b) captures the dual variable of the last pair in a chain. Since $\lambda_v \in \mathbb{R}_+$ for all $v \in \mathcal{V}$ (see (LR3) in

the Online Appendix), thus, if the dual variable of a given vertex $v \in \mathcal{V}$ is large enough to lead to a negative-price path at node \mathbf{t} , we may need to cut that path short at some previous vertex in the sequence to obtain a positive-price chain. For instance, in Figure 3b consider $\lambda_2 = \lambda_3 = 5$, all the other dual variables set to zero and $w_{uv} = 1$ for all $(u, v) \in \mathcal{A}$. Sequence $(4, 1, 5)$ representing a 2-length chain in $\tilde{\mathcal{D}}^i$ is contained in $(4, 1, 5, 3)$. Clearly, the former yields the highest reduced cost of a chain in Figure 3b. Thus, $\bar{\eta}^i = \bar{\eta}^i((n_4, n_5)) = 2$. Next, we show a series of results on the complexity of computing a positive-price column via MDDs. The corresponding proofs are presented in the Online Appendix C.

PROPOSITION 4. Given the reduced costs \hat{r}_c^i and \bar{r}_p^i expressed as an arc-separable function for all $(n_s, n_{s'}) \in \hat{\mathcal{A}}^i$ and $(n_s, n_{s'}) \in \bar{\mathcal{A}}^i$, a positive-price cycle, if one exists, can be found in time $\mathcal{O}(\sum_{i \in \hat{I}} \sum_{(n_s, n_{s'}) \in \hat{\mathcal{A}}^i} |\delta_-^i(n_s)|)$. Similarly, a positive-price chain can be found in $\mathcal{O}(\sum_{i \in \bar{I}} \sum_{(n_s, n_{s'}) \in \bar{\mathcal{A}}^i} |\delta_-^i(n_s)|)$.

PROPOSITION 5. The size of the input $\sum_{i \in \hat{I}} \sum_{(n_s, n_{s'}) \in \hat{\mathcal{A}}^i} |\delta_-^i(n_s)|$ grows as $|\hat{\mathcal{V}}^i|^{K+1}$ does.

PROPOSITION 6. The size of the input $\sum_{i \in \bar{I}} \sum_{(n_s, n_{s'}) \in \bar{\mathcal{A}}^i} |\delta_-^i(n_s)|$ grows as $|\bar{\mathcal{V}}^i|^{L+2}$ does for bounded chains and as $|\bar{\mathcal{V}}^i|!$ when $L \rightarrow \infty$.

Despite potentially very large diagram sizes in general, there are three reasons for which finding a positive-price column can still be done efficiently in practice. First, even though $|\mathcal{V}|$ can be large, arc density of \mathcal{D} for real KEP instances is below 50% (Saidman et al. 2006, Anderson et al. 2015, Dickerson et al. 2016). Second, for small values of K and L , it is possible to reduce considerably the size of the input by selecting appropriately a K -limited FVS. Lastly, MDDs are reduced significantly after the state transition graph is obtained (Cire and van Hoeve 2013).

4.4. Branching scheme

The search tree may have exponential depth when branching is done on possibly every cycle, thus, branching on arcs is usually preferred. If \mathcal{D} is a complete graph, there can be up to $|\mathcal{P}||\mathcal{P} - 1| + |\mathcal{P}||\mathcal{N}|$ arcs in \mathcal{A} . On the other hand, branching on arcs in $\hat{\mathcal{A}}^i$ and $\bar{\mathcal{A}}^i$ implies that there are up to $(|\bar{I}| + |\hat{I}|)|\mathcal{P}||\mathcal{P} - 1| + |\bar{I}||\mathcal{P}||\mathcal{N}|$ arcs across all graph copies. Among the two arc-based schemes,

branching on arcs in \mathcal{A} results in a lower depth branching tree. We therefore choose this option as our branching scheme.

Particularly, on every fractional node of the search tree we branch on an arc $(u, v) \in \mathcal{A}$ whose fractional value is closest to 0.5. That is, we generate two children, one in which the arc is prohibited and another in which the arc is selected. When banning an arc from the RMP, we modify Equation (2b) by replacing w_{uv} with a sufficiently large negative number M . By doing so, the length of any path in any copy traversing that arc approaches negative infinity, thereby ruling it out due to the definition of $\hat{\eta}^i$ and $\bar{\eta}^i$. On the other hand, enforcing an arc $(u, v) \in \mathcal{A}$ requires the inclusion of the following constraint in the RMP:

$$\sum_{i \in \bar{I}} \sum_{c \in \mathcal{C}_K^i: (u,v) \in \mathcal{A}(c)} z_c^i + \sum_{i \in \bar{I}} \sum_{p \in \mathcal{C}_L^i: (u,v) \in \mathcal{A}(p)} z_p^i = 1 \quad (\mu_{(u,v)}) \quad (4)$$

The addition of constraint (4) changes the reduced cost of a chain and cycle. If we let $\mathcal{A}^* \subseteq \mathcal{A}$ be the set of selected arcs in a branch-and-bound node, the reduced cost of a column in the i th MDD, is now given by

$$\hat{r}_c^i = w_c - \sum_{v \in \mathcal{V}(c)} \lambda_v - \sum_{(u,v) \in \mathcal{A}^* \cap \mathcal{A}(c)} \mu_{(u,v)} \quad c \in \mathcal{C}_K^i \quad (5a)$$

$$\bar{r}_p^i = w_p - \sum_{v \in \mathcal{V}(p)} \lambda_v - \sum_{(u,v) \in \mathcal{A}^* \cap \mathcal{A}(p)} \mu_{(u,v)} \quad p \in \mathcal{C}_L^i \quad (5b)$$

where $\mu_{(u,v)}$ is the dual variable of Constraint (4). Thus, if $(val(a'), val(a)) \in \mathcal{A}^*$, then $\mu_{(val(a'), val(a))}$ can be subtracted from recursive expression (2b) to account for Constraint (4) in the RMP.

If the solution of the RMP is fractional, we branch, and then apply column generation to the resulting node. After optimally solving the RMP, the upper bound given by its objective value is compared to the best lower bound found. If the former is lower, that branch is pruned. Otherwise, a lower bound is obtained by granting integrality to the decision variables (columns) in the RMP and re-solving it. Whenever a lower bound matches the best upper bound, optimality is achieved. If, due to time limitations, it is not possible to solve the RMP to optimality, (LR-UB) provides a valid upper bound on the optimal value of the KEP, as presented next.

4.5. A New Upper Bound on the Optimal Objective Value of the KEP

In this section, we propose what to the best of our knowledge is the only other known upper bound on the optimal objective value of the KEP, which is tighter than the existing proposed bound (Abraham et al. 2007), while recent works provide no upper bound for instances that timed out (Lam and Mak-Hau 2020). The upper bound in Abraham et al. (2007) consists of solving an unrestricted maximum weight matching problem ($K = L = \infty$) on a bipartite graph, which can be solved in polynomial time. Our new upper bound (LR-UB), based on Lagrangian relaxation, is particularly useful when the optimality of the RMP cannot be proven within the time limit:

$$\mathcal{Z}(\lambda) = \sum_{i \in \bar{I}} \hat{\mathcal{Z}}^i(\lambda) + \sum_{i \in \hat{I}} \bar{\mathcal{Z}}^i(\lambda) + \sum_{u \in \mathcal{V}} \lambda_u \quad (\text{LR-UB})$$

where λ_u corresponds to the dual variables of Constraints (1a) in IDCF, and $\hat{\mathcal{Z}}^i(\lambda)$ and $\bar{\mathcal{Z}}^i(\lambda)$ correspond to the pricing problems (CC) and (CH) in Online Appendix A, respectively. We refer the reader to Appendix A for an explanation of how λ_u are decision variables in a Lagrangian relaxation and for a formal proof on the validity of (LR-UB).

5. General Solution Framework

In our solution framework, a combination of exact and restricted MDDs is used so that once built they are stored in computer memory and retrieved every time pricing problems need to be solved. As a result, we cannot solely rely on MDDs to prove optimality of the RMP. We introduce a three-phase solution framework consisting of a search through MDDs for both cycles and chains (Phase 1), a cutting plane algorithm to search for positive-price chains and cycles, whose final goal is to prove that no more positive-price chains exist (Phase 2), and a two-step search to find a positive-price cycle, if any (Phase 3). Figure 4 illustrates the framework.

5.1. Phase 1: Solving the pricing problems via MDDs

Building the MDDs is the first step. We parameterize some aspects to make a reasonable usage of computer memory (Section 6). Particularly, if $K \geq 4$ and $|\mathcal{P}| > 500$, we build restricted MDDs by considering a maximum cycle length of 3 in 90% of the decision diagrams, while in the remaining

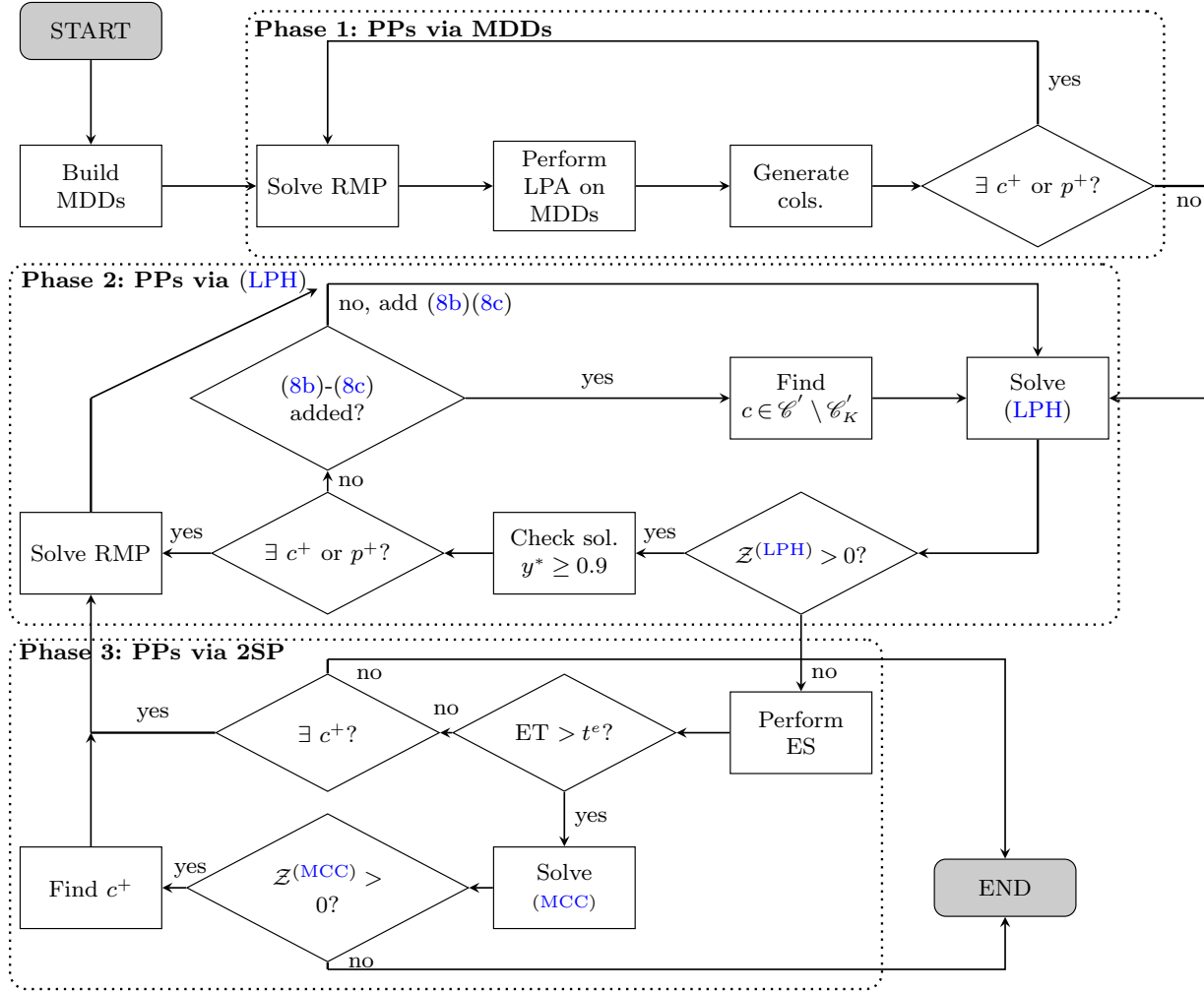


Figure 4 Flow chart of column generation for $K \geq 3$, $L \in \mathbb{Z}_+$. PPs stands for pricing problems, LPA for longest-path algorithm, cols. for columns, ES for exhaustive search, ET for elapsed time, c^+ (p^+) for positive-price cycle (chain), and 2SP for the two-step procedure described in Phase 3.

10% we keep the true value of K . If $K \leq 4$ and $|\mathcal{P}| \leq 500$, we build exact MDDs. When constructing a transition state graph for chains, we explore at most 20% of vertices receiving an arc from $v \in \mathcal{V}$, unless $|\mathcal{N}| > 250$, in which case we explore only 10%. In all cases, the maximum length of chains (in terms of arcs) considered in the construction of MDDs is also 3, regardless of the true value of L . After the MDDs are built, we store them in memory and use them to solve the pricing problems as depicted by Figure 4, in integration with Phases 2 and 3.

5.2. Phase 2: A longest path formulation for chains and cycles

We use a longest path problem as a relaxation of (CH) in which the goal is to find an \mathbf{s} - \mathbf{t} path or a cycle, both corresponding to feasible positive-price columns. To this end, let us define $\mathcal{D}' = (\mathcal{V}', \mathcal{A}')$ as a digraph whose vertex set $\mathcal{V}' = \mathcal{V} \cup \{\mathbf{s}, \mathbf{t}\}$ has two dummy vertices \mathbf{s} and \mathbf{t} such that the set of arcs $\mathcal{A}' = \mathcal{A} \cup \{(\mathbf{s}, u) \cup (v, \mathbf{t}) \mid u \in \mathcal{N}, v \in \mathcal{P}\}$ connects dummy vertex \mathbf{s} to NDDs and PDPs to vertex \mathbf{t} . For arcs including a dummy vertex, their weight is set to zero. Moreover, let \mathcal{C}' be the set of all simple cycles and $\mathcal{C}'_K \subseteq \mathcal{C}'$ be the set of feasible cycles in \mathcal{D}' . As defined before, \mathcal{A}^* is the set of selected arcs. A decision variable y_{uv} takes the value 1 if arc $(u, v) \in \mathcal{A}'$ is selected, and 0 otherwise. Thus, a relaxed longest path formulation at some node in the branching tree is

$$\mathcal{Z}^{(\text{LPH})} := \max \sum_{(u,v) \in \mathcal{A}': u \neq \mathbf{s}} (w_{uv} - \lambda_u) y_{uv} - \sum_{(u,v) \in \mathcal{A}^*} \mu_{(u,v)} y_{uv} \quad (\text{LPH})$$

$$\text{s.t.} \quad \sum_{v:(u,v) \in \mathcal{A}'} y_{uv} - \sum_{v:(v,u) \in \mathcal{A}'} y_{vu} = \begin{cases} 1, & u = \mathbf{s} \\ 0, & u \in \mathcal{V} \\ -1, & u = \mathbf{t} \end{cases} \quad (7a)$$

$$\sum_{(u,v) \in \mathcal{A}'} y_{uv} \leq 1 \quad u \in \mathcal{V} \quad (7b)$$

$$y_{uv} \in [0, 1] \quad (u, v) \in \mathcal{A}' \quad (7c)$$

Although a solution of (LPH) may lead to a path using more than L arcs, or a solution with subtours, or a non-integer solution, we see these downsides as an opportunity to either find efficiently a positive-price chain (cycle) missed in the first phase or prove that none exists. Because (LPH) is a relaxation of (CH), whenever the objective value of (LPH) is zero, so is the objective value of (CH). Note that even without subtour-elimination constraints, a solution of (LPH) guarantees a path (may be fractional) from vertex \mathbf{s} to \mathbf{t} due to flow-balance Constraints (7a). The solution may also have subtours representing positive-price cycles useful for the RMP. Particularly, if y^* is an optimal solution of (LPH), we check arcs $(u, v) \in \mathcal{A}'$ for which $y_{uv}^* \geq 0.9$ when searching for positive-price columns. Lastly, enforcing two dummy arcs, one going out of \mathbf{s} and one coming into \mathbf{t} ,

requires us to adjust the right-hand side of Constraints (8b), resulting in the following constraints:

$$\sum_{(u,v) \in c} y_{uv} \leq |c| - 1 \quad c \in \mathcal{C}' \setminus \mathcal{C}'_K \quad (8a)$$

$$\sum_{(u,v) \in \mathcal{A}'} y_{uv} \leq L + 2 \quad (8b)$$

$$y_{uv} \in \{0, 1\} \quad (u, v) \in \mathcal{A}' \quad (8c)$$

Therefore, the goal is to solve first a linear program without Constraints (8), check the solution for positive-price and *feasible* columns, and only then add (8) if need be. Experimentally, we observed that the “warmed-up” dual variables resulting from Phase 1 allow us to relax integrality constraints and yet obtain an integer solution in many cases. Figure 4 shows how (LPH) + Constraints (8) is solved via a cutting plane algorithm integrated with the other two phases during column generation.

5.3. Phase 3: A two-step procedure for cycles

If a positive-price cycle still exists in \mathcal{D} but not found in Phases 1 and 2, we perform an exhaustive enumeration of cycles while the time limit is not exceeded. Otherwise, the exhaustive search ends and a MIP is solved instead. Note that Phase 2 guarantees to find any positive-price chain, if does exists. Therefore, in Phase 3, we only have to search positive-price cycles.

5.3.1. Exhaustive search We perform a depth-first search on every cycle copy $\hat{\mathcal{G}}^i$, where a feasible cycle is rooted at $v_i^* \in \mathcal{V}^*$. First, we sort and search over the graph copies in increasing order of their λ_v values. Next, we traverse $\hat{\mathcal{G}}^i$, and when v_i^* is the leaf node of a path from the root and it is found at a position between 3 and $K + 1$, that path constitutes a feasible cycle c . If $\hat{r}_c^i > 0$, the cycle has a positive reduced cost and it is sent to the RMP. [Abraham et al. \(2007\)](#) and [Lam and Mak-Hau \(2020\)](#) implemented a similar search, although unlike them, our paths are rooted at vertices in FVS. Despite of searching cycles on trees rooted only at a subset of vertices, exhaustive enumeration becomes a bottleneck for large instances. Therefore, whenever a time threshold, t^e , is surpassed we shift to solving the MIP provided next.

5.3.2. A MIP for cycles (MCC) finds a feasible cycle in \mathcal{D} with maximum reduced cost at some branch-and-bound node. If found, the cycle is sent to the RMP. Note that Constraint (9c) guarantees at most K selected arcs, whether they are distributed in multiple (smaller) cycles or not. Thus, there is no need for subtour-elimination constraints. (MCC) is formulated as follows:

$$\mathcal{Z}^{(\text{MCC})} = \max \sum_{(u,v) \in \mathcal{A}} (w_{uv} - \lambda_u) y_{uv} - \sum_{(u,v) \in \mathcal{A}^*} \mu_{(u,v)} y_{uv} \quad (\text{MCC})$$

$$\text{s.t.} \quad \sum_{v:(u,v) \in \mathcal{A}} y_{uv} - \sum_{v:(v,u) \in \mathcal{A}} y_{vu} = 0 \quad u \in \mathcal{V} \quad (9a)$$

$$\sum_{v:(u,v) \in \mathcal{A}} y_{uv} \leq \begin{cases} 1, & u \in \mathcal{P} \\ 0, & u \in \mathcal{N} \end{cases} \quad (9b)$$

$$\sum_{(u,v) \in \mathcal{A}} y_{uv} \leq K \quad (9c)$$

$$y_{uv} \in \{0, 1\} \quad (u, v) \in \mathcal{A} \quad (9d)$$

5.3.3. Algorithmic details In the three-phase solution framework given in Figure 4, after building the MDDs, the pricing problems are solved to optimality as follows. During Phase 1, we compute $\hat{\eta}^i$ and $\bar{\eta}^i$ for all $i \in \bar{I}$ and $i \in \hat{I}$, respectively, and add the positive-price columns found to the RMP after every iteration. We encourage the use of chains by returning up to 15 positive-price chain columns to the RMP, whereas only one from every cycle MDD. Note that in both cases, recursions (3a)-(3b) only need to be computed once. In Phase 2, we delay the inclusion of Constraints (8), until their addition is mandatory to find a positive-price chain column. Every time a solution is checked during Phase 2, a positive-price cycle column is searched when failing to find a chain column. As for Phase 3, we set $t^e = 20$ s to exhaustively find a positive-price cycle or reach the end with none. If the time threshold is exceeded, we proceed to solve (MCC) and resolve the RMP, if needed. When there are no NDDs present in the input graph \mathcal{D} , we simply skip Phase 2. Likewise, since MDDs are exact when $K \leq 4$, $|\mathcal{P}| \leq 500$ and no NDDs, Phases 2 and 3 are also dropped. Lastly, note that the procedure given in Figure 4 can be easily adapted to the case $L = \infty$, since it suffices to remove Constraint (8b).

6. Computational Experiments

Our code base and test instances are publicly available at <https://github.com/d-aleman/KEP-BPMDD>. MDDs as well as our B&P algorithm (BP_MDD) are implemented in C++ and experiments are conducted on a machine with Debian GNU/Linux as operating system and a 3.60GHz processor Intel(R) Core(TM) with 120 GB RAM, of which we allocated a maximum of 8 GB for BP_MDD (including the construction of MDDs) and 60 GB for state-of-the-art solution methods. CPLEX 12.10 is used as the LP/MIP solver. We investigate the extent up to which leading approaches could scale in practice, therefore, we allocated a larger RAM capacity. BP_MDD is compared against the state-of-the-art PICEF and HPIEF solution methods (Dickerson et al. 2016). The PICEF and HPIEF solvers are retrieved from the original authors, where HPIEF is the model with full reduction. They call Gurobi 7.5.2 to solve MIP models. Although different LP/MIP solvers may add noise to the analysis, in the latest history of benchmark sets, Gurobi is the lead (Mittelman 2020). It is worth noting that Lam and Mak-Hau (2020) hold the state-of-the-art solver for the cycle-only version. They tested their algorithm on the same library as ours, PrefLib (Mattei and Walsh 2013), achieving total run-times up to 33s for instances with 2048 PDPs and mostly less than a second for instances with 1024 PDPs, when $K = 3$. For $K = 4$ with 1024 PDPs, their maximum run-time among the 9 instances optimally solved was 21.8min. The total run-time of our algorithm, although small, is larger than that reported by Lam and Mak-Hau (2020), particularly when $K = 3$. However, since Lam and Mak-Hau (2020) did not consider larger values of K , and their approach is for cycles only, we do not compare to them in this analysis. When $L = 0$, the formulation by McElfresh et al. (2019) reduces to the cycle formulation, and so does PICEF. Therefore, we compare BP_MDD with HPIEF and PICEF, which we refer to as “solvers”.

6.1. Instances

For our subsequent analysis, we used the PrefLib repository (Mattei and Walsh 2013), whose instances were generated by Dickerson et al. (2012) based on data from KPDPs in the United States. The first group, referred to as KEP_N0, has 80 instances, split into 8 subsets, each

with 10 instances and no NDDs; and hence, only cycles are considered. In this group, $|\mathcal{P}| \in \{16, 32, 64, 128, 256, 512, 1024, 2048\}$ and their arc density varies from 10% to 32%.

The second group of instances, referred to as `KEP_N`, is split into 23 subsets with 10 instances in each. NDDs are present, thus, both cycles and chains are considered in the solution. For these instances, $16 \leq |\mathcal{P}| \leq 2048$, $1 \leq |\mathcal{N}| \leq 307$ and the arc density is within 23% and 46%.

6.2. Computational performance

PICEF, HPIEF and BP_MDD are evaluated on the two groups of instances. Each instance in `KEP_N0` is solved for $K \in \{3, 4, 5, 6\}$, totaling 320 runs per solver. For `KEP_N`, we set $K \in \{3, 4\}$ and $L \in \{3, 4, 5, 6\}$. The total number of runs per solver in this second group is very large, $10 \times 23 \times 2 \times 4 = 1840$ runs. Therefore, we proceed as follows: For each run, if the RAM usage exceeds the limit, the solver stops and aborts the rest of instances in that run's subset, which we presume would lead to the same memory issues. Regardless of the group, for every run we set a time limit of 30min. Only one thread was used for all the experiments and the rule to find the K -limited FVS is the maximum in-degree. An analysis on multiple criteria to obtain a K -limited FVS from Algorithm 1 and their implications on performance and scalability is presented in the Online Supplement D.

Figure 5 plots the number of instances in `KEP_N0` solved to optimality up to discrete points in time before reaching the 30-min limit, which shows the outperformance of our algorithm over the state of the art. The time reported includes both the total MDD construction time and the B&P algorithm time.

When $K = 3$, BP_MDD and PICEF solve all 80 instances in under 20min, followed by HPIEF under 26min. When $K \in \{4, 5, 6\}$, BP_MDD solves all 80 instances under 25min. Both PICEF and HPIEF perform poorly as K increases. RAM usage of BP_MDD did not exceed 4 GB in these experiments, while PICEF and HPIEF surpassed 60 GB. Instances that run out of memory accumulated more than 37 million variables. By definition PICEF is exponential in the number of variables, thus, this result is not surprising. However, HPIEF is polynomial in terms of the number of variables and constraints, even more so the full-reduction HPIEF we compare our algorithm against, and yet dimensionality is clearly a challenge.

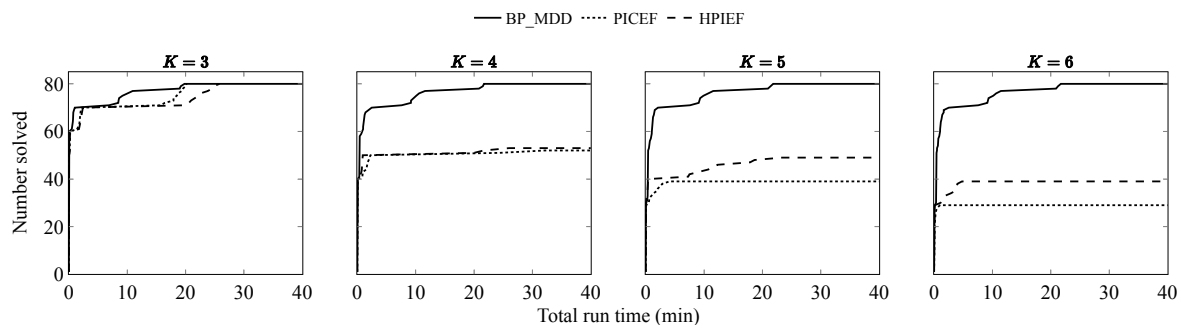


Figure 5 Performance profiles for the set `KEP_N0`.

In 94% of runs, BP_MDD solves instances to optimality at the root node and at most 8 nodes are explored in the branch-and-bound tree. On average, for instances with $|\mathcal{P}| \geq 1024$, 55% of the total run-time accounts for solving the pricing problems, with a minimum and maximum percentage of 19% and 84%, respectively. Phase 3 is responsible on average for 27% (range: [5%, 72%]) of the pricing time when $K \geq 4$. On the same runs ($|\mathcal{P}| \geq 1024$ and $K \geq 4$), the average and maximum time for building the MDDs is 109.8s and 257.5s, respectively. For only 10 instances with $K \geq 4$, PICEF and HPIEF report a feasible solution within the time limit, meaning that for the others the RAM threshold is exceeded. The optimality gap reported by these solvers varies between 0% and 30%, with respect to the best solution found among all the three solvers. Overall, PICEF is slightly better than HPIEF in terms of optimality gap but not in terms of the number of instances that could fit into memory.

Figure 6 shows the solution time (without preprocessing or MDD construction) taken for every run and the state-of-the-art solver when $K \in \{3, 4\}$ for all chain lengths. Markers above the diagonal indicate BP_MDD is faster. Particularly, BP_MDD is faster in 20% of runs when $|\mathcal{P}| < 512$, yet the maximum run-time taken for BP_MDD to solve these instances is < 4 s. When $|\mathcal{P}| \geq 512$, BP_MDD is faster in 80% of runs.

Figure 7 shows the performance profiles for the instances in `KEP_N` solved to optimality by the three solvers, which demonstrates that our algorithm outperforms the others, especially when long chains are allowed. For $K = 3$ and $L = 3$, the performance at the time limit is similar for

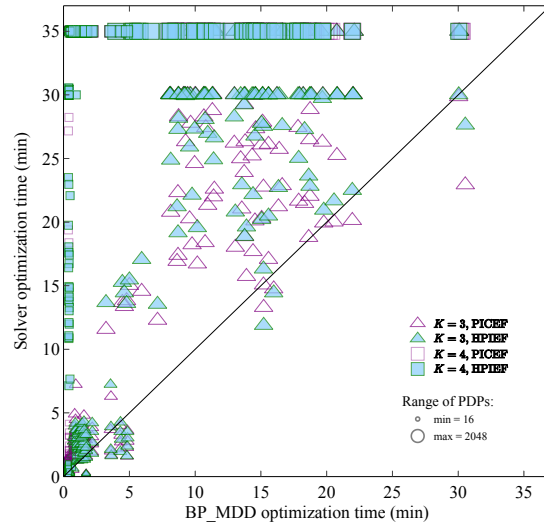


Figure 6 Performance comparison when $L \in \{0, 3, 4, 5, 6\}$ and $K = 3$ (triangles) and $K = 4$ (squares). The size of the markers indicate the number of PDPs in the instances. Markers located at the y -axis value of 35 on the top of the plot indicate instances that were not solved to optimality within the time limit.

the three algorithms, although BP_MDD does not solve one instance (2048 PDPs and 307 NDDs) to optimality. For that instance, BP_MDD's optimality gap is 0.2%. The same instance remains suboptimal across the other K - L combinations. The performance of PICEF and HPIEF decreases as K and L increases. The maximum optimality gap provided by PICEF and HPIEF, among the 95 suboptimal runs at the time limit is 11%. Among these two solvers, HPIEF provided 67% of the suboptimal solutions.

On average, BP_MDD solved 94% of runs to optimality at the root node, with a maximum of two explored branch-and-bound nodes. For instances with $|\mathcal{P}| \geq 1024$, solving the pricing problems accounts for 66% of the total run-time, and on average 53% of the pricing time is spent in Phase 1. For the same instances, the time spent on building the MDDs accounts on average for 25% of the total run-time, with a maximum of 35%. On average, in more than 90% of the cases, all NDDs were used in the final solution. Lastly, we note that the majority of columns across all runs are found in Phase 1 (Online Supplement D).

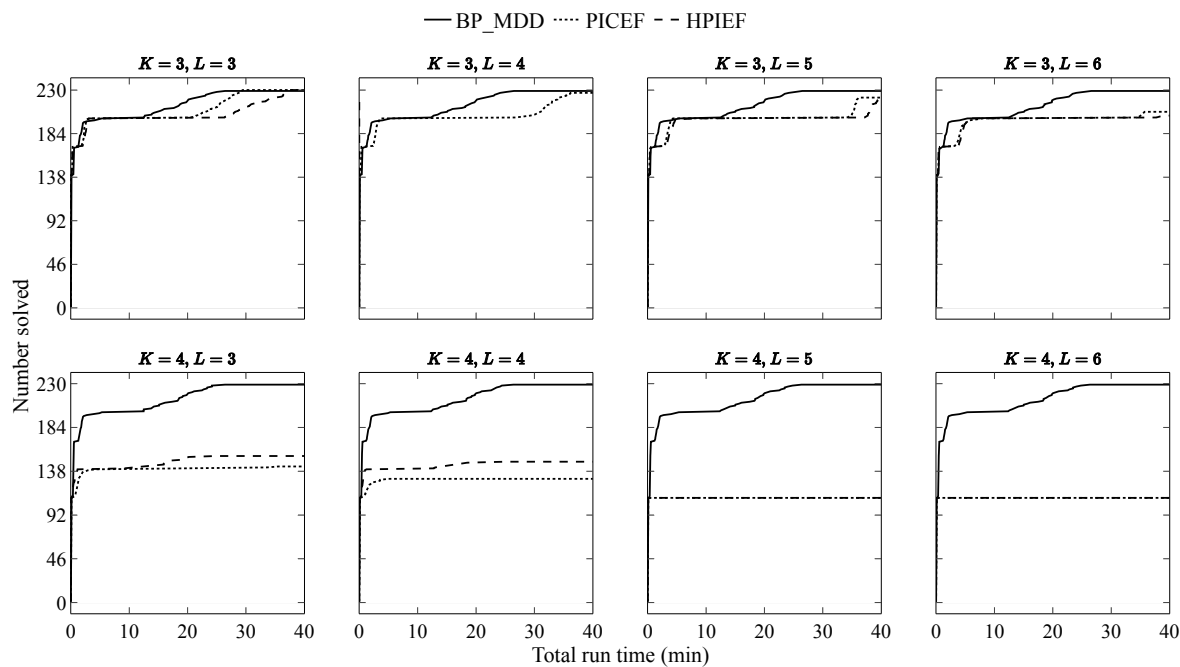


Figure 7 Number of instances solved for set KEP_N .

6.3. Sensitivity analysis on the solution structure

In this section, we first investigate the benefit of long chains for different instance structures, according to the presence of highly sensitized patients. In the second part of our analysis, we show the change in the composition of different optimal solutions when cycles are prioritized over chains and vice versa. To the best of our knowledge, BP_MDD is the only exact algorithm for which such a preference can be selected a priori.

6.3.1. The value of long chains An important question from a practical perspective is, whether the same optimal matching value achieved when allowing chains can be obtained by relying only on cycles, and thus disregarding the need of chains. [Ashlagi et al. \(2012\)](#) and [Dickerson et al. \(2012\)](#) showed analytically that, when the graph is sufficiently sparse, chains benefit the number of matched patients. A standard methodology to study this practical question is the use of analytical models. These models, generate random graphs, e.g., vertices and arcs, by following probability estimates on inherent characteristics to KPDP participants, such as a patient’s sensitization degree and the number of highly-sensitized patients in the graph. For our further analysis, we use a similar

random graph model to that of [Ashlagi et al. \(2012\)](#) and [Ding et al. \(2018\)](#). Particularly, we also assume the existence of two patient-donor pair categories: highly-sensitized and low-sensitized. Instead of building completely random graphs, we take a sample of instances from `KEP_N` and preserve arcs $(u, v) \in \mathcal{A}$ with probability p_h if the patient (and thus the pair) in vertex v is highly-sensitized or probability p_ℓ if that patient is not. Our goal is to perform a sensitivity analysis on the original instances. Therefore, in [Figure 8](#) we use the notation (σ, p_ℓ) to represent an instance where the proportion of low-sensitized pairs over the total number of pairs is σ and p_ℓ is the compatibility probability for low-sensitized pairs. In all cases, we set $p_h = 5\%$, taken from [Ding et al. \(2018\)](#).

We selected 3 small-size instances (indexed by S-181, S-182 and S-183) and 3 medium-size instances (indexed by M-201, M-202, M-203) from the group `KEP_N`. The former have 256 pairs and 38 singleton donors whereas the latter have 512 pairs and 25 singleton donors. For each instance, we generated 6 random graphs according to the tuples (σ, p_ℓ) depicted in [Figure 8](#). The average graph densities from left to right are 4.2%, 6.8%, 5.6%, 9.2%, 8.9% and 15.7%. Overall, the higher the percentage of low-sensitized patients, the higher the arc density.

These instances were solved within an optimality gap of $\leq 3\%$, with 93.5% solved under $\leq 1\%$ optimality gap. Overall, these instances are substantially more challenging. `BP_MDD` solved optimally 57% of them in 151.9 seconds, on average. The feasible solutions took on average 1850.3 seconds, with the largest solution time exceeding an hour.

The empirical results depicted in [Figure 8](#) complement previous findings on the benefit of chains ([Ashlagi et al. 2012](#), [Dickerson et al. 2012](#), [Ding et al. 2018](#)). For sparse graphs, chains, particularly long chains (involving more than three transplants) are able to reach more patients when the opportunities of cyclic exchanges are scarce. In all cases there is a significant benefit from a cycle-only solution to one allowing chains of size at least three. Chains become shorter, stabilizing around three, as the percentage of low-sensitized patients increase. This behavior is also observed for the vast majority of instances in `KEP_N`, which are significantly denser than the ones presented in [Figure 8](#). On average, each instance in `KEP_N` sees an increase of 20% when passing from a solution

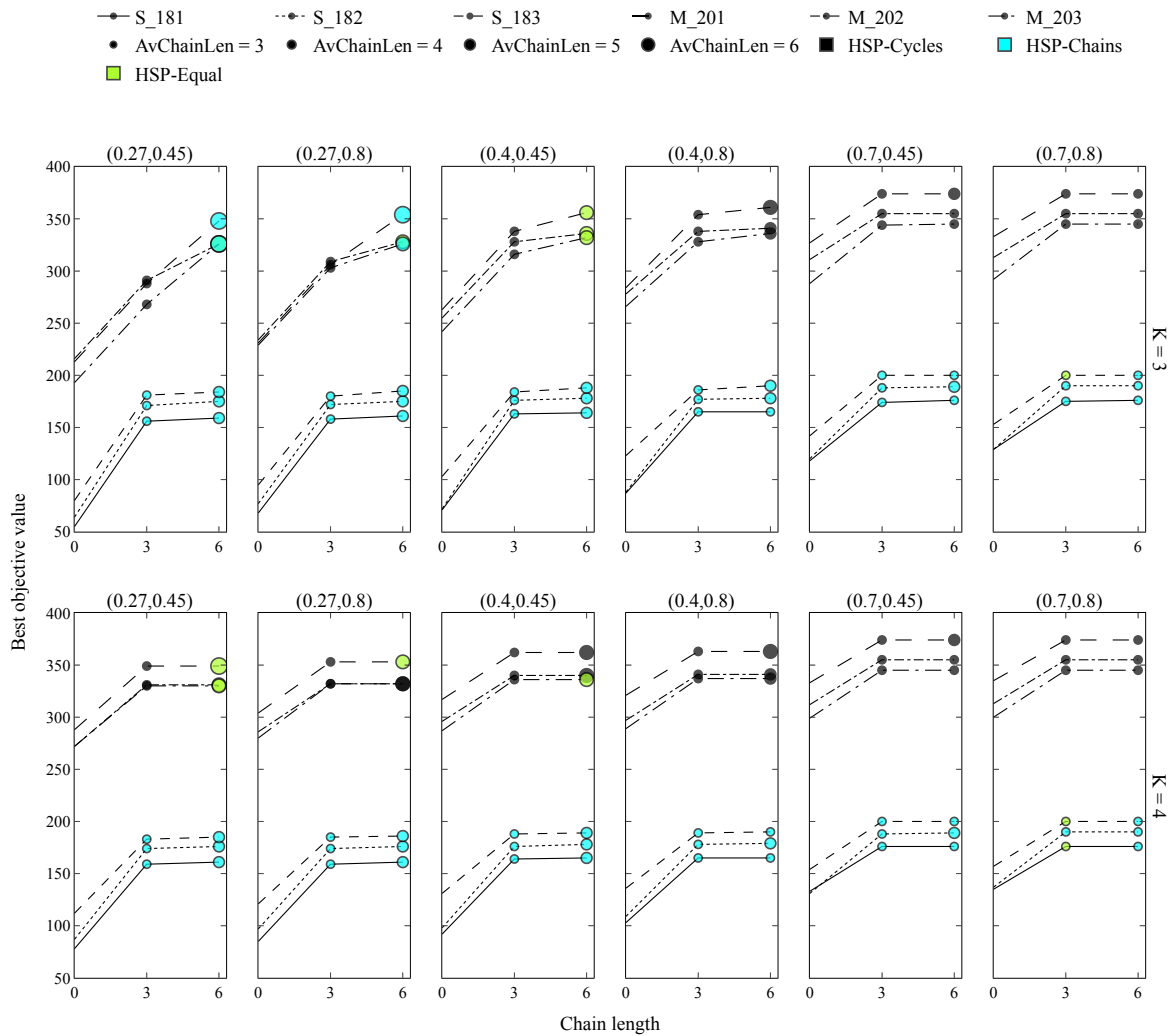


Figure 8 Change in the number of matches by sensitization category and chain length. **AvChainLen**: average chain length of an instance solution, rounded to the closest integer; **HSP-Chains (Cycles)**: chains (cycles) included a higher percentage of the matched and highly sensitized patients; **HSP-Equal**: difference between the percentage of matched and highly-sensitized patients in chains and cycles is less than 5%.

with $K = 3$ and no chains to one with $K = L = 3$, and about 19% from no chains and $K = 4$ to $K = 4, L = 3$. From this point on, increasing the size of chains beyond three, seems only significant for a handful of the small and medium size instances.

For the small size instances in Figure 8, allowing chains seem to be critical to include the difficult to match patients in a solution, even when the arc density increases. When the length of cycles is four, chains still provide benefit, although it seems that an important number of pairs that were

reached before by long chains can be matched in these long cycles. Interestingly, chains seem to have a more dramatic effect as the size of the instances increase.

6.3.2. Solution composition under prioritization by exchange type Another relevant question is, whether for the same optimal matching value, one can opt for a solution that prioritizes the presence of chains over cycles or vice versa. For instance, chains can be prioritized over cycles since even when failures occur in arcs or vertices of the graph, the original chain can simply turn into a shorter one, whereas a cyclic exchange falls apart altogether (Klimentova et al. 2016, Dickerson et al. 2019).

With this concern in mind, we added two modes under which BP_MDD can be executed. The default mode, referred to as “CH”, prioritizes chains over cycles and corresponds to returning up to 15 positive-price chain columns to the RMP, as described in Section 5.3.3. The alternative mode, referred to as “CY”, prioritizes cycles over chains by restricting the number of chain columns returned to the RMP at every iteration of the column generation algorithm to up most one.

We note that in CH mode, there is no guarantee that the optimal solution will use the largest number of patients matched through chains. Since the prioritization of chains is encouraged by adding positive-price chains over positive-price cycles, whenever a positive-price chain is encountered, thus, the optimal base of the RMP has more possibilities to build a KEP solution with as many chains as possible, but this solution (although optimal) may or may not match the largest number of patients through chains. In CY mode, since the size of a K-limited FVS is generally much larger than the number of singleton donors (Online Supplement D), there is a high chance of discovering a larger number of positive-price cycle columns, as opposed to those corresponding to chains. Therefore, if possible, the resulting feasible solution consists mostly of cycles.

To compare the impact of prioritizing chains (CC) or cycles (CY), Table 1 shows the average chain and cycle length and number of cycles for the instances shown in Figure 8. It is worth noting that *all* singleton donors were used under both modes. Under CH mode, BP_MDD finds longer chains and fewer cycles. In both cases, the length of cycles remains steady around three. The

Table 1 Solution composition by chain (CH) and cycle (CY) prioritization modes. Data is aggregated by the small and medium size instances in Figure 8 and cycle lengths $K = \{3, 4\}$.

(σ, p_ℓ)	L	CH, CY mode average			Average CH/CY ratio		
		Chain length	Cycle length	# cycles	Chain length	Cycle length	# cycles
(0.27,0.45)	3	2.93, 2.91	3.08, 3.09	46.25, 46.67	1.01	1.00	0.99
(0.27,0.45)	6	4.65, 4.45	2.93, 2.90	37.33, 40.58	1.06	1.01	0.81
(0.27,0.8)	3	2.92, 2.79	2.99, 2.78	50.58, 52.50	1.05	1.00	0.93
(0.27,0.8)	6	4.47, 4.25	2.88, 2.82	40.42, 44.75	1.08	1.02	0.79
(0.4,0.45)	3	2.93, 2.84	2.96, 2.95	54.75, 56.08	1.04	1.00	0.95
(0.4,0.45)	6	4.35, 4.05	2.80, 2.84	44.08, 48.33	1.09	0.98	0.83
(0.4,0.8)	3	2.89, 2.67	2.91, 2.86	57.58, 61.17	1.09	1.02	0.90
(0.4,0.8)	6	3.91, 3.36	2.84, 2.80	49.33, 56.67	1.19	1.01	0.78
(0.7,0.45)	3	2.85, 2.46	2.82, 2.78	64.08, 70.25	1.18	1.01	0.86
(0.7,0.45)	6	3.41, 2.73	2.79, 2.75	58.75, 68.00	1.26	1.02	0.78
(0.7,0.8)	3	2.85, 2.30	2.84, 2.82	64.33, 71.75	1.29	1.02	0.83
(0.7,0.8)	6	3.19, 2.54	2.83, 2.83	60.92, 69.17	1.30	1.00	0.80

difference in the chain length becomes more evident as the instances become denser. The same overall behavior is observed in set KEP_N (Online Supplement D).

Due to the possible presence of multiple optima, the average length of chains should be analyzed in context. The prioritization of chains through the CH mode in Table 1 can be seen as a guidance on what the average length of chains could be if we were to implement a solution that mostly consists of chains. Conversely, when prioritizing cycles over chains, we obtain optimal solutions consisting of smaller chains and more cycles.

In terms of computational performance, the solution time for KEP_N instances under the CY mode, was on average 8 times slower when compared to CH. This result can be explained due to the restriction on chain columns in the RMP. Thus, forcing BP_MDD to go over more iterations to prove optimality of the RMP. Moreover, about 90% of the KEP_N instances under the CY mode were solved to optimality. The average gap was 0.3%.

Note that BP_MDD can be extended to encompass other priorities. It is known that highly-sensitized patients tend to wait longer for a match offer than those who are not. If exchanges of a given size are preferred, the longest path for the MDDs can focus on finding, if any, positive-price chains (cycles) among the targeted exchanges. Phases two and three also offer alternatives to choose which and how many of those exchanges to return to the RMP. These prioritization schemes work

in a similar fashion to having hierarchical objectives (Glorie et al. 2014), with the advantage that multiple runs of the algorithm are not required.

7. Conclusion

We addressed the problem of finding a matching in kidney exchange, considering long chains, and developed a novel B&P framework in which the pricing problems for both cycles and chains are primarily solved via MDDs. We note that our framework is, to the best of our knowledge, the only exact algorithm for KEP in which a preference for cycles or chains can be selected a priori by decision-makers and the first correct B&P algorithm for the cycles-and-chains variant (Omer et al. 2022), as well proved a new Lagrangian-based valid upper bound to the problem. This framework showed significant improved computational performance over current state-of-the-art methods, though differences in programming language (Python for Dickerson et al. (2016) and C++ for us) prevent a true apples-to-apples comparison despite using the same computational environment. While our B&P framework is presented specifically for KEP—as all B&P implementations are bespoke—it can be adapted to any problem of detecting cycles and chains in a network (e.g., variations of the travelling salesman problem), or where the pricing problem can be formulated as an MDD.

A limitation of restricted decision diagrams is that they only include a subset of the cycles or chains that may be needed in the restricted master problem, thus, the use of the additional phases is still required for arbitrary cycle and chain lengths. For future work, we will develop a simulation to examine the performance of our approach over multiple matching epochs to assess long-term real-world utility, and consider metrics such as maximum time to transplant, with special attention on outcomes for highly-sensitized patients. We note consideration of time to transplant and other priority rules can be incorporated into the current framework as objective function weights, as the objective function is already weighted per patient.

Finally, a significant barrier to implementation of mathematically-driven decision-making in healthcare applications is complexity of the optimization techniques. In some applications, a web-based tool or other UIUX can help adoption of mathematically complex decision-making tools, but

in Canada, just like in other countries, the KPDPs operators are typically appointed to government-run institutions that have their own regulations on clinical data treatment and other protocols that are unique to the specific needs of a KPDP, and thus, a web tool may not be highly valued from an implementation perspective. However, such a tool could be used to communicate the value of investing in high performance optimization software and personnel to administrative decision-makers; thus, development of a front-end tool is another direction of future work.

Acknowledgments

References

- Abraham DJ, Blum A, Sandholm T (2007) Clearing algorithms for barter exchange markets: Enabling nationwide kidney exchanges. *Proceedings of the 8th ACM conference on Electronic commerce*, 295–304.
- Alvelos F, Klimentova X, Viana A (2019) Maximizing the expected number of transplants in kidney exchange programs with branch-and-price. *Annals of Operations Research* 272:429–444.
- Anderson R, Ashlagi I, Gamarnik D, Roth AE (2015) Finding long chains in kidney exchange using the traveling salesman problem. *Proceedings of the National Academy of Sciences* 112(3):663–668.
- Ashlagi I, Gamarnik D, Rees MA, Roth AE (2012) The need for (long) chains in kidney exchange. Working paper, National Bureau of Economic Research.
- Ashlagi I, Roth AE (2021) Kidney exchange: An operations perspective. *Management Science* 67(9):5455–5478.
- Awasthi P, Sandholm T (2009) Online stochastic optimization in the large: Application to kidney exchange. *IJCAI International Joint Conference on Artificial Intelligence*, 405–411.
- Barnhart C, Johnson EL, Nemhauser GL, Savelsbergh MWP, Vance PH (1998) Branch-and-Price: Column Generation for Solving Huge Integer Programs. *Operations Research* 46(3):316–329.
- Biró P, Haase-Kromwijk B, Andersson T, Ásgeirsson EI, Baltsová T, Boletis I, Bolotinha C, Bond G, Bóhmig G, Burnapp L, Cechlárová K, Di Ciaccio P, Fronek J, Hadaya K, Hemke A, Jacquelinet C, Johnson R, Kieszek R, Kuypers DR, Leishman R, Macher MA, Manlove D, Menoudakou G, Salonen M, Smeulders B, Sparacino V, Spieksma FC, Valentín MO, Wilson N, van der Klundert J (2019) Building Kidney Exchange Programmes in Europe—An Overview of Exchange Practice and Activities. *Transplantation* 103:1514–1522.
- Biró P, van de Klundert J, Manlove D, Pettersson W, Andersson T, Burnapp L, Chromy P, Delgado P, Dworzak P, Haase B, Hemke A, Johnson R, Klimentova X, Kuypers D, Costa AN, Smeulders B, Spieksma F, Valentín MO, Viana A (2021) Modelling and optimisation in European Kidney Exchange Programmes. *European Journal of Operational Research* 291(2):447–456.

-
- Canadian Blood Services (2019) Interprovincial organ sharing national data report: Kidney Paired Donation Program 2009–2018. Technical report, Canadian Blood Services, https://professionaleducation.blood.ca/sites/default/files/kpd-eng_2018.pdf.
- Cantwell L, Woodroffe C, Holdsworth R, Ferrari P (2015) Four years of experience with the Australian kidney paired donation programme. *Nephrology (Carlton, Vic.)* 20(3):124–131.
- Carvalho M, Klimentova X, Glorie K, Viana A, Constantino M (2020) Robust models for the kidney exchange problem. *INFORMS Journal on Computing* 33(3):861–881.
- Castro MP, Cire AA, Beck JC (2020) An MDD-based Lagrangian approach to the multicommodity pickup-and-delivery TSP. *INFORMS Journal on Computing* 32(2):263–278.
- CIHI (2019) Annual statistics on organ replacement in Canada: Dialysis, transplantation and donation, 2009 to 2018. Ottawa, ON: CIHI; 2019. Technical report, Canadian Institute for Health Information, <https://www.cihi.ca/sites/default/files/document/corr-snapshot-2019-en.pdf>.
- Cire AA, van Hoeve WJ (2013) Multivalued decision diagrams for sequencing problems. *Operations Research* 61(6):1411–1428.
- Constantino M, Klimentova X, Viana A, Rais A (2013) New insights on integer-programming models for the kidney exchange problem. *European Journal on Operations Research* 231(1):57–68.
- Delorme M, García S, Gondzio J, Kalcsics J, Manlove D, Pettersson W, Trimble J (2022) Improved instance generation for kidney exchange programmes. *Computers & Operations Research* 141:105707.
- Dickerson JP (2014) Robust dynamic optimization with application to kidney exchange. *Proceedings of the 2014 International Conference on Autonomous Agents and Multi-Agent Systems*, 1701–1702 (Richland, SC: International Foundation for Autonomous Agents and Multiagent Systems).
- Dickerson JP, Manlove DF, Plaut B, Sandholm T, Trimble J (2016) Position-indexed formulations for kidney exchange. *Proceedings of the 2016 ACM Conference on Economics and Computation*, 25–42.
- Dickerson JP, Procaccia AD, Sandholm T (2012) Optimizing kidney exchange with transplant chains: Theory and reality. *Proceedings of the 11th International Conference on Autonomous Agents and Multiagent Systems - Volume 2*, 711–718.
- Dickerson JP, Procaccia AD, Sandholm T (2019) Failure-aware kidney exchange. *Management Science* 65(4):1768–1791.
- Ding Y, Ge D, He S, Ryan CT (2018) A nonasymptotic approach to analyzing kidney exchange graphs. *Operations Research* 66(4):918–935.
- Flechner SM, Thomas AG, Ronin M, Veale JL, Leeser DB, Kapur S, Peipert JD, Segev DL, Henderson ML, Shaffer AA, Cooper M, Hil G, Waterman AD (2018) The first 9 years of kidney paired donation through the National Kidney Registry: Characteristics of donors and recipients compared with National Live Donor Transplant Registries. *American Journal of Transplantation* 18(11):2730–2738.

- Glorie KM, van de Klundert JJ, Wagelmans APM (2014) Kidney exchange with long chains: An efficient pricing algorithm for clearing barter exchanges with branch-and-price. *Manufacturing & Service Operations Management* 16(4):498–512.
- Hooker JN (2013) Decision diagrams and dynamic programming. *Integration of AI and OR Techniques in Constraint Programming for Combinatorial Optimization Problems*, 94–110 (Springer).
- Karp R (1972) *Reducibility among combinatorial problems*, 85–103 (Boston, MA: Springer).
- Kinable J, Cire AA, van Hoesel WJ (2017) Hybrid optimization methods for time-dependent sequencing problems. *European Journal on Operations Research* 259(3):887–897.
- Klimentova X, Alvelos F, Viana A (2014) A new branch-and-price approach for the kidney exchange problem. *Computational Science and Its Applications – ICCSA 2014*, 237–252 (Springer).
- Klimentova X, Pedroso JaP, Viana A (2016) Maximising expectation of the number of transplants in kidney exchange programmes. *Computers & Operations Research* 73:1–11.
- Klimentova X, Viana A, Pedroso JP, Santos N (2021) Fairness models for multi-agent kidney exchange programmes. *Omega* 102:102333.
- Lam E, Mak-Hau V (2020) Branch-and-cut-and-price for the cardinality-constrained multi-cycle problem in kidney exchange. *Computers & Operations Research* 115.
- Mak-Hau V (2015) On the kidney exchange problem: cardinality constrained cycle and chain problems on directed graphs: a survey of integer programming approaches. *Journal of Combinatorial Optimization* 33(1):35–39.
- Malik S, Cole E (2014) Foundations and Principles of the Canadian living donor paired exchange program. *Canadian Journal of Kidney Health and Disease* 1(1):6.
- Mattei N, Walsh T (2013) Preflib: A Library for Preferences <http://www.preflib.org>. Perny P, Pirlot M, Tsoukiàs A, eds., *Algorithmic Decision Theory*, 259–270 (Berlin, Heidelberg: Springer Berlin Heidelberg).
- McElfresh D, Bidkhorji H, Dickerson J (2019) Scalable robust kidney exchange. *Proceedings of the AAAI Conference on Artificial Intelligence* 33:1077–1084.
- Mittelman HD (2020) Benchmarking optimization software—a (Hi)story. *SN Operations Research Forum* 1(2).
- Monteiro T, Klimentova X, Pedroso JP, Viana A (2021) A comparison of matching algorithms for kidney exchange programs addressing waiting time. *Central European Journal of Operations Research* 29(2):539–552.
- Omer J, Arslan AN, Yan F (2022) KidneyExchange.jl: A Julia package for solving the kidney exchange problem with branch-and-price. <https://hal.inria.fr/hal-03830810/document>.
- Plaut B, Dickerson J, Sandholm T (2016a) Hardness of the pricing problem for chains in barter exchanges. <https://arxiv.org/abs/1606.00117>.

-
- Plaut B, Dickerson JP, Sandholm T (2016b) Fast Optimal Clearing of Capped-Chain Barter Exchanges. *Proceedings of the Thirtieth AAAI Conference on Artificial Intelligence*, 601–607 (AAAI Press).
- Raghunathan AU, Bergman D, Hooker J, Serra T, Kobori S (2018) Seamless multimodal transportation scheduling. <https://arxiv.org/abs/1807.09676>.
- Rees MA, Dunn TB, Kuhr CS, Marsh CL, Rogers J, Rees SE, Cicero A, Reece LJ, Roth AE, Ekwenna O, Fumo DE, Krawiec KD, Kopke JE, Jain S, Tan M, Paloyo SR (2017) Kidney exchange to overcome financial barriers to kidney transplantation. *American Journal of Transplantation* 17(3):782–790.
- Roth AE, Sönmez T, Ünver MU (2007) Efficient kidney exchange: Coincidence of wants in markets with compatibility-based preferences. *American Economic Review* 97(3):828–851.
- Saidman SL, Roth AE, Sönmez T, Ünver MU, Delmonico FL (2006) Increasing the opportunity of live kidney donation by matching for two- and three-way exchanges. *Transplantation* 5(81):773–82.
- Trapianti CN (2022) Al via programma di trapianti incrociati di rene tra Italia e Usa, firmato l'accordo. *Centro Nazionale Trapianti* URL <https://www.trapianti.salute.gov.it/trapianti/dettaglioComunicatiNotizieCnt.jsp?lingua=italiano&area=cnt&menu=media&sottomenu=news&id=784>.
- Wall AE, Veale JL, Melcher ML (2018) Advanced donation programs and deceased donor-initiated chains-2 Innovations in kidney paired donation. *Transplantation* 101(12):2818–2824.

Appendix

A. Pricing Problems and New Valid Upper Bound

We introduce a Lagrangian decomposition of the KEP based on an improved and generalized version of an existing integer programming (IP) formulation. Particularly, we show that the Lagrangian decomposition leads to (i) an IP formulation for the pricing problems and (ii) a new valid upper bound on the optimal value of the KEP that can be used in B&P and is stronger than the other existing bound (Abraham et al. 2007). Lastly, we show an advantage of using the *disaggregated cycle formulation* (Klimentova et al. 2014) over the so-called *cycle formulation* (Abraham et al. 2007, Roth et al. 2007) in B&P.

A.1. IEEF: An Improved Extended Edge Formulation (EEF)

For the cycle-only version of the KEP, Constantino et al. (2013) cloned the input digraph \mathcal{D} , $|\mathcal{P}|$ times, drawn by the fact that $|\mathcal{P}|$ is a natural upper bound on the number of cycles in any feasible solution. The idea is then to find a feasible cycle in each copy of \mathcal{D} . If the selected cycles across the copies are vertex-disjoint, they represent a feasible matching. Thus, an IP formulation can be built based on this disaggregation of \mathcal{D} to solve the problem. We extend this formulation by including long chains and reducing the number of copies. To this end, we start by showing that any *feedback vertex set* (FVS) provides a valid upper bound on the number of vertex-disjoint cycles in \mathcal{D} , whose proof is omitted due to its simplicity.

DEFINITION 4. Given a directed graph $\mathcal{D} = (\mathcal{V}, \mathcal{A})$, $\mathcal{V}^* \subseteq \mathcal{V}$ is a feedback vertex set of \mathcal{D} if the subgraph induced by $\mathcal{V} \setminus \mathcal{V}^*$ is acyclic.

PROPOSITION 1. Given a digraph $\mathcal{D} = (\mathcal{V}, \mathcal{A})$, let n be the cardinality of the set with the maximum number of vertex-disjoint cycles in \mathcal{D} , and \mathcal{V}^* be an FVS. Then, $n \leq |\mathcal{V}^*|$.

The goal is to create one cycle copy per every vertex in the FVS. We use Algorithm 1 to this end, except that now, we replace the function `BuildMDD` in line 8 by a function that creates a digraph associated to the corresponding feedback vertex. Because our extension includes chains,

we also create copies of the input graph for chains, one for every NDD. We can now introduce our extension of the extended edge formulation, which will provide us with a mechanism to compute a valid upper bound on the maximum number of matches.

Let \bar{I} denote the index set of chain copies, with $|\bar{I}| \leq |\mathcal{N}|$. The i -th chain copy of \mathcal{D} , $i \in \bar{I}$, is represented by graph $\bar{\mathcal{D}}^i = (\bar{\mathcal{V}}^i, \bar{\mathcal{A}}^i)$, whose vertex set $\bar{\mathcal{V}}^i = \mathcal{P} \cup \{u_i, \tau\}$ is formed by all PDPs, the i -th NDD, u_i , and a dummy vertex τ , representing a dummy patient receiving a fictitious donation from the paired donor in the last pair of a chain. The set of arcs $\bar{\mathcal{A}}^i = (\mathcal{A} \setminus \{(u, v) \in \mathcal{A} \mid u \in \mathcal{N} \setminus u_i, v \in \mathcal{P}\}) \cup \{(v, \tau) \mid v \in \mathcal{P}\}$ removes arcs emanating from NDDs other than u_i and adds one dummy arc from every PDP to τ . Thus, a chain can only be started by the NDD u_i on the i th chain copy. Additionally, let $\bar{\mathcal{C}}^i$ and $\bar{\mathcal{C}}_K^i \subseteq \bar{\mathcal{C}}^i$ be the set of all simple cycles and the set of all feasible cycles in $\bar{\mathcal{D}}^i$, respectively. Lastly, let \hat{x}_{uv}^i and \bar{x}_{uv}^i be decision variables taking the value 1 if arc $(u, v) \in \hat{\mathcal{A}}^i$ and arc $(u, v) \in \bar{\mathcal{A}}^i$ is selected in a cycle and chain, respectively, and 0 otherwise. Then, the improved extended edge formulation is formulated as follows:

$$\max \sum_{i \in \bar{I}} \sum_{(u,v) \in \hat{\mathcal{A}}^i} w_{uv} \hat{x}_{uv}^i + \sum_{i \in \bar{I}} \sum_{(u,v) \in \bar{\mathcal{A}}^i} w_{uv} \bar{x}_{uv}^i \quad (\text{IEEF})$$

$$\text{s.t.} \quad \sum_{i \in \hat{I}} \sum_{(u,v) \in \hat{\mathcal{A}}^i} \hat{x}_{uv}^i + \sum_{i \in \bar{I}} \sum_{(u,v) \in \bar{\mathcal{A}}^i} \bar{x}_{uv}^i \leq 1 \quad u \in \mathcal{V} \quad (10a)$$

$$\sum_{v:(u,v) \in \hat{\mathcal{A}}^i} \hat{x}_{uv}^i = \sum_{v:(v,u) \in \hat{\mathcal{A}}^i} \hat{x}_{vu}^i \quad i \in \hat{I}, u \in \hat{\mathcal{V}}^i \quad (10b)$$

$$\sum_{v:(u,v) \in \bar{\mathcal{A}}^i} \bar{x}_{uv}^i = \sum_{v:(v,u) \in \bar{\mathcal{A}}^i} \bar{x}_{vu}^i \quad i \in \bar{I}, u \in \bar{\mathcal{V}}^i \setminus \{u_i, \tau\} \quad (10c)$$

$$\sum_{(u,v) \in \hat{\mathcal{A}}^i} \hat{x}_{uv}^i \leq K \quad i \in \hat{I} \quad (10d)$$

$$\sum_{(u,v) \in \bar{\mathcal{A}}^i} \bar{x}_{uv}^i \leq L \quad i \in \bar{I} \quad (10e)$$

$$\sum_{v:(u,v) \in \hat{\mathcal{A}}^i} \hat{x}_{uv}^i \leq \sum_{v:(v_i^*, v) \in \hat{\mathcal{A}}^i} \hat{x}_{v_i^* v}^i \quad i \in \hat{I}; u \neq v_i^* \quad (10f)$$

$$\sum_{v:(u,v) \in \bar{\mathcal{A}}^i} \bar{x}_{uv}^i \leq \sum_{v:(u_i, v) \in \bar{\mathcal{A}}^i} \bar{x}_{u_i v}^i \quad i \in \bar{I}; u \in \bar{\mathcal{V}}^i \setminus \{u_i, \tau\} \quad (10g)$$

$$\sum_{(u,v) \in \mathcal{A}(c)} \bar{x}_{uv}^i \leq |\mathcal{V}(c)| - 1 \quad i \in \bar{I}, c \in \bar{\mathcal{C}}^i \setminus \bar{\mathcal{C}}_K^i \quad (10h)$$

$$\hat{x}_{uv}^i \in \{0, 1\} \quad i \in \hat{I}, (u, v) \in \hat{\mathcal{A}}^i \quad (10i)$$

$$\bar{x}_{uv}^i \in \{0, 1\} \quad i \in \bar{I}, (u, v) \in \bar{\mathcal{A}}^i \quad (10j)$$

The objective function maximizes the weighted sum of transplant scores. Constraints (10a) enforce that a donor (paired or single) donates at most one kidney. Constraints (10b) guarantee that in a selected cycle copy, if a PDP receives a kidney, then it donates one to another pair in the same copy. Constraints (10c) ensure that in a chain if a patient in a PDP receives a kidney, his or her paired donor donates either to a PDP in the same chain or to a dummy vertex, as it is the case of the donor in the last PDP of the chain. Constraints (10d) and (10e) limit the number of arcs in a cycle to K and the number of arcs in a chain to L in a copy, respectively. Constraints (10f) forbid the use of the i -th cycle copy unless the i -th vertex in the FVS, v_i^* , is selected in that copy. Likewise, constraints (10g) allow the use of the i -th chain copy only when the singleton donor, u_i , triggers a chain. The presence of cycles (subtours) in chain copies, particularly of those with size higher than K , jeopardize the correctness of the formulation. Therefore, constraints (10h) ensure the elimination of all infeasible cycles from chain copies. These constraints resemble those used in the recursive formulation of Anderson et al. (2015), except that their arc variables are based on the input graph in a model allowing arbitrarily long chains. We note that Constantino et al. (2013) and Klimentova et al. (2014) did not consider infeasible-cycle-breaking constraints in their discussion on how to include NDDs in the EEF, and thus can be deemed incomplete. Infeasible-cycle-breaking constraints, e.g., Constraints (10h), are *necessary* to preserve the correctness of the EEF, and thus that of IEEF. A counter example showing the need of such constraints in EEF to allow chains and a formal proof for Proposition 2 are provided in Section C.

PROPOSITION 2. *IEEF is a correct formulation of the matching problem in the KEP.*

A.2. Lagrangian relaxation

Consider introducing the following valid (redundant) constraints to (IEEF):

$$\sum_{(u,v) \in \hat{\mathcal{A}}^i} \hat{x}_{uv}^i \leq 1 \quad i \in \hat{I}, u \in \hat{\mathcal{V}}^i \quad (11a)$$

$$\sum_{(u,v) \in \mathcal{A}^i} \bar{x}_{uv}^i \leq 1 \quad i \in \bar{I}, u \in \mathcal{V}^i \quad (11b)$$

Before justifying these new constraints, let us first approximate the optimal objective value of (IEEF) by relaxing constraints guaranteeing at most one donation from every donor Constraints (10a) and then penalizing their violation by imposing Lagrange multipliers (λ) in the objective function. This relaxation may allow a vertex to be selected in more than one graph copy, thus, in more than one exchange. However, if a copy is selected, such a vertex can be selected at most once within that copy, due to Constraints (11). Given $\lambda \in \mathbb{R}_+^{|\mathcal{V}|}$, a Lagrangian relaxation to the KEP can be formulated as follows:

$$\begin{aligned} \mathcal{Z}(\lambda) := & \quad (LR1) \\ \max & \sum_{i \in \hat{I}} \sum_{(u,v) \in \mathcal{A}^i} w_{uv} \hat{x}_{uv}^i + \sum_{i \in \bar{I}} \sum_{(u,v) \in \mathcal{A}^i} w_{uv} \bar{x}_{uv}^i + \sum_{v \in \mathcal{V}} \lambda_v \left(1 - \sum_{i \in \hat{I}} \sum_{(u,v) \in \mathcal{A}^i} \hat{x}_{uv}^i + \sum_{i \in \bar{I}} \sum_{(u,v) \in \mathcal{A}^i} \bar{x}_{uv}^i \right) \\ \text{s.t.} & \quad (10b) - (10j), (11a) - (11b) \quad (12a) \end{aligned}$$

As the only constraints linking decision variables associated with different copies are now relaxed, (LR1) can be decomposed by graph copies as follows:

$$\mathcal{Z}(\lambda) = \sum_{i \in \hat{I}} \hat{\mathcal{Z}}^i(\lambda) + \sum_{i \in \bar{I}} \bar{\mathcal{Z}}^i(\lambda) + \sum_{u \in \mathcal{V}} \lambda_u \quad (LR2)$$

where, $\forall i \in \hat{I}$ and $\forall i \in \bar{I}$, we have the following subproblems, respectively:

$$\hat{\mathcal{Z}}^i(\lambda) := \max \left\{ \sum_{(u,v) \in \mathcal{A}^i} (w_{uv} - \lambda_u) \hat{x}_{uv}^i \mid (10b), (10d), (10f), (10i), (11a) \right\}, \quad (CC)$$

$$\bar{\mathcal{Z}}^i(\lambda) := \max \left\{ \sum_{(u,v) \in \mathcal{A}^i} (w_{uv} - \lambda_u) \bar{x}_{uv}^i \mid (10c), (10e), (10h), (10j), (11b) \right\}. \quad (CH)$$

Given a set of Lagrange multipliers, λ , each subproblem finds either a feasible cycle, (CC), or a feasible chain, (CH), whose vertex assignment has minimum penalty, thus, maximum weight. Observe that the inclusion of the dummy vertex τ is useful to capture the Lagrange multiplier of the last pair in a chain in the objective function of (CH). The Lagrangian dual problem can

be defined as $\sigma^{LD} := \min\{\mathcal{Z}(\lambda) : \lambda \in \mathbb{R}_+^{|\mathcal{V}|}\}$. That is, σ^{LD} is the smallest upper bound that can be obtained when the set of Lagrange multipliers favor an assignment of vertices to cycle and chain copies with minimum intersection. If we define \mathcal{Z}^{LP} as the optimal objective value of the linear programming relaxation of (IEEF), it is possible that $\sigma^{LD} < \mathcal{Z}^{LP}$. Moreover, we show that the quality of the bound provided by σ^{LD} is as tight as the one provided by the linear programming relaxation of the disaggregated cycle formulation (Klimentova et al. 2014), one of the formulations in the literature providing the tightest linear relaxation.

PROPOSITION 3. *If \mathcal{Z}_c^{LP} is the optimal objective value of the linear programming relaxation of the disaggregated cycle formulation, then $\sigma^{LD} = \mathcal{Z}_c^{LP}$.*

Proof. Let $\hat{\mathcal{C}}_K^i$ and $\bar{\mathcal{C}}_L^i$ be the set of feasible cycles (including vertex v_i^*) and chains on the i th graph copy, $i \in \hat{I}, i \in \bar{I}$, respectively. For a cycle $c \in \hat{\mathcal{C}}_K^i$ and chain $p \in \bar{\mathcal{C}}_L^i$, let $w_c = \sum_{(u,v) \in \mathcal{A}(c)} w_{uv}$ and $w_p = \sum_{(u,v) \in \mathcal{A}(p)} w_{uv}$ be the total weight of a cycle and chain, respectively. Then, (LR2) is reformulated as follows:

$$\min \sum_{i \in \bar{I}} \hat{\mathcal{Z}}^i + \sum_{i \in \hat{I}} \bar{\mathcal{Z}}^i + \sum_{v \in \mathcal{V}} \lambda_v \quad (\text{LR3})$$

$$\hat{\mathcal{Z}}^i \geq w_c - \sum_{v \in \mathcal{V}(c)} \lambda_v \quad i \in \hat{I}, c \in \hat{\mathcal{C}}_K^i \quad (z_c^i) \quad (14a)$$

$$\bar{\mathcal{Z}}^i \geq w_p - \sum_{v \in \mathcal{V}(p)} \lambda_v \quad i \in \bar{I}, p \in \bar{\mathcal{C}}_L^i \quad (z_p^i) \quad (14b)$$

$$\hat{\mathcal{Z}}^i \geq 0 \quad i \in \hat{I} \quad (14c)$$

$$\bar{\mathcal{Z}}^i \geq 0 \quad i \in \bar{I} \quad (14d)$$

$$\lambda_v \geq 0 \quad v \in \mathcal{V} \quad (14e)$$

(LR3) finds the optimal value of decision variables $\hat{\mathcal{Z}}^i$, $\bar{\mathcal{Z}}^i$ and λ . The validity of (LR3) relies on the fact that the maximum weight cycle and chain is selected for every graph copy through Constraints (14a) and (14b), met in the equality by the minimization objective. Moreover, since the objective value of (CC) and (CH) can at least be zero (by selecting $\hat{x} = 0$ and $\bar{x} = 0$), Constraints

(14c) and (14d) represent a valid lower bound on the objective value of each sub-problem. To finalize the proof, letting z_c^i and z_p^i be the dual variables of constraints (14a) and (14b), respectively, the dual problem of (LR3) is

$$\max \sum_{i \in \hat{I}} \sum_{c \in \hat{\mathcal{C}}_K^i} w_c z_c^i + \sum_{i \in \bar{I}} \sum_{p \in \bar{\mathcal{C}}_L^i} w_p z_p^i \quad (\text{IDCF})$$

$$\sum_{i \in \hat{I}} \sum_{c \in \hat{\mathcal{C}}_K^i : v \in \mathcal{V}(c)} z_c^i + \sum_{i \in \bar{I}} \sum_{p \in \bar{\mathcal{C}}_L^i : v \in \mathcal{V}(p)} z_p^i \leq 1 \quad v \in \mathcal{V} \quad (15a)$$

$$z_c^i \geq 0 \quad i \in \hat{I}, c \in \hat{\mathcal{C}}_K^i \quad (15b)$$

$$z_p^i \geq 0 \quad i \in \bar{I}, p \in \bar{\mathcal{C}}_L^i \quad (15c)$$

Note that Constraints $\sum_{c \in \hat{\mathcal{C}}_K^i} z_c^i \leq 1 \quad \forall i \in \hat{I}$ are omitted from (IDCF) along with their chain counterpart since they are implied by Constraints (15a). Formulation (IDCF) corresponds to the integer linear programming relaxation of the *disaggregated cycle formulation* in Klimentova et al. (2014), noting that in (IDCF) chain variables are included and cycle copies are found through Algorithm 1. Hence, by strong duality it follows that $\sigma^{LD} = \mathcal{Z}_c^{LP}$. \square

Notice that by enforcing integrality of the decision variables, (IDCF) becomes a valid formulation for the matching problem in kidney exchange, similar to the so-called cycle formulation (Abraham et al. 2007, Roth et al. 2007), except that cycles and chains are not found in specific graph copies. Thus, the i index is dropped. It had not been shown before whether there is an advantage to using one formulation over another, particularly for B&P. Note that the dual variables of Constraints (15a) correspond to the Lagrange multipliers λ in (LR2). Thus, the subproblems in the Lagrangian relaxation, (CC) and (CH), correspond to the pricing problems for the RMP based on IDCF. Moreover, this result shows that when cycles and chains are disaggregated into graph copies, it is possible to obtain a valid upper bound on the objective value by solving (CC) and (CH), and simply plugging their result into (LR2) afterwards. Even if the set of Lagrange multipliers is not optimal, (LR2) provides a valid upper bound, which can be as good as that of the disaggregated cycle formulation or the cycle formulation itself. Thus, even without proving optimality of (IDCF),

its dual variables can still be used to obtain a valid upper bound. To the best of our knowledge, the only previous method in the literature obtaining a valid upper bound consists of solving a relaxed problem with $K = L = \infty$ (Abraham et al. 2007), which can be solved in polynomial time. It is easy to see that the bound provided by this special case is weaker than that of the presented Lagrangian dual problem. Since (IDCF) can be used as a master problem in column generation, the goal is to use the bound provided by (LR2) when it is not possible to prove optimality of the master problem. In Section 4.4, we show how this new upper bound can be used not just at every node of a branch-and-bound tree.

B. On the completeness of two existing formulations

In this section, we present the edge assignment formulation and the extended edge formulation including NDDs, as proposed by Constantino et al. (2013). We show that for these formulations to model chains correctly, the inclusion of infeasible-cycle-breaking constraints is required.

B.1. Edge Assignment Formulation

Following an equivalent notation to that used by Constantino et al. (2013), we proceed to introduce some notation. Let $D = (V, A)$ be a digraph representing compatibilities among donors (single or paired) and PDPs. The set of vertices $V = \{1, \dots, |\mathcal{P}| + |\mathcal{N}|\}$ has $|\mathcal{P}|$ -many PDPs and $|\mathcal{N}|$ -many NDDs. Let vertices $\{1, \dots, |\mathcal{N}|\}$ represent NDDs and vertices $\{|\mathcal{N}| + 1, \dots, |\mathcal{N}| + |\mathcal{P}|\}$ represent PDPs. An arc $(i, j) \in A$ exists if the donor in vertex i is compatible with patient in vertex j . Assume that a dummy patient is associated to each NDD, so that paired donors $j \in \{|\mathcal{N}| + 1, \dots, |\mathcal{N}| + |\mathcal{P}|\}$ are compatible with each dummy patient $i \in \{1, \dots, |\mathcal{N}|\}$. Also, consider $|V|$ as an upper bound on the number of cycles and chains in any feasible solution. For each vertex $\ell \in \{|\mathcal{N}| + 1, \dots, |\mathcal{P}| + |\mathcal{N}|\}$, let $V^\ell = \{i \in V \mid i \geq \ell\}$ be the set of vertices forming cycles with index higher or equal to ℓ , whereas for each index $\ell \in \{1, \dots, |\mathcal{N}|\}$ let $V^\ell = \{i \in \mathcal{P}\} \cup \{\ell\}$ be the set of vertices forming part of a chain started by the ℓ -th NDD. Notice that only vertices $i \geq \ell$ are included in each vertex set to remove multiplicity of solutions. Moreover, it can happen that for some $\ell \in \{1, \dots, |V|\}$, $V^\ell = \emptyset$, e.g., if all vertices pointing or receiving an arc from the vertex with the lowest index are removed. Thus,

denote by \mathcal{L} the set of indices for which $V^\ell \neq \emptyset$. Lastly, consider the following binary decision variables: x_{ij} takes on value 1 if arc (i, j) is selected in a cycle or chain and y_i^ℓ takes on value 1 if node i is assigned to the ℓ th cycle or chain. Then, the edge assignment formulation is defined as follows:

$$\max \sum_{(i,j) \in A} w_{ij} x_{ij} \tag{16a}$$

$$\sum_{j:(j,i) \in A} x_{ji} = \sum_{j:(i,j) \in A} x_{ij} \quad i \in V \tag{16b}$$

$$\sum_{j:(i,j) \in A} x_{ij} \leq 1 \quad i \in V \tag{16c}$$

$$\sum_{i \in \{\ell\} \cup \{|\mathcal{N}|+1, \dots, |\mathcal{P}|+|\mathcal{N}|\}} y_i^\ell \leq L \quad \ell \in \{1, \dots, |\mathcal{N}|\} \tag{16d}$$

$$\sum_{i \geq |\mathcal{N}|+1} y_i^\ell \leq K \quad \ell \in \{|\mathcal{N}|+1, \dots, |\mathcal{N}|+|\mathcal{P}|\} \tag{16e}$$

$$\sum_{\ell \in \mathcal{L}: i \in V^\ell} y_i^\ell = \sum_{j:(i,j) \in A} x_{ij} \quad i \in V \tag{16f}$$

$$y_i^\ell + x_{ij} \leq 1 + y_j^\ell \quad (i, j) \in A, \ell \in \mathcal{L}, i \in V^\ell \tag{16g}$$

$$y_i^\ell \leq y_\ell^\ell \quad \ell \in \mathcal{L}, i \in V^\ell \tag{16h}$$

$$y_i^\ell \in \{0, 1\} \quad \ell \in \mathcal{L}, i \in V^\ell \tag{16i}$$

$$x_{ij} \in \{0, 1\} \quad (i, j) \in A \tag{16j}$$

Constraints (16b) assure that patient i receives a kidney if and only if donor j donates a kidney. Constraints (16c) allow at most one donation. Constraints (16d) and (16e) limit the length of chains and cycles. Constraints (16f) ensure that vertex i is in a cycle (chain) if and only if there is an assignment of i to some ℓ . Constraints (16g) state that if vertex i is in cycle (chain) ℓ and donor i gives a kidney to recipient j , then vertex j must also be in the ℓ -th cycle (chain). Constraints (16h) establish that a vertex $i \in V^\ell$ can be assigned to the ℓ -th cycle (chain) only if vertex ℓ is also assigned. Constraints (16i) and (16j) indicate decision variables' domain.

Now, we proceed to show a solution example satisfying (16) and yet infeasible to the KEP. Consider Figure 9 and assume $K = 3$ and $L = 6$. Notice that in the solution, $y_2^2 = y_3^2 = y_4^2 = y_5^2 = y_6^2 = y_3^3 = y_4^3 = y_5^3 = y_6^3 = y_4^4 = y_5^4 = y_6^4 = y_5^5 = y_6^5 = x_{46} = x_{54} = x_{56} = x_{65} = x_{52} = x_{62} = x_{26} = 0$ and $y_1^1 = y_2^1 = y_3^1 = y_4^1 = y_5^1 = y_6^1 = x_{53} = x_{36} = x_{64} = x_{45} = x_{12} = x_{21} = 1$.

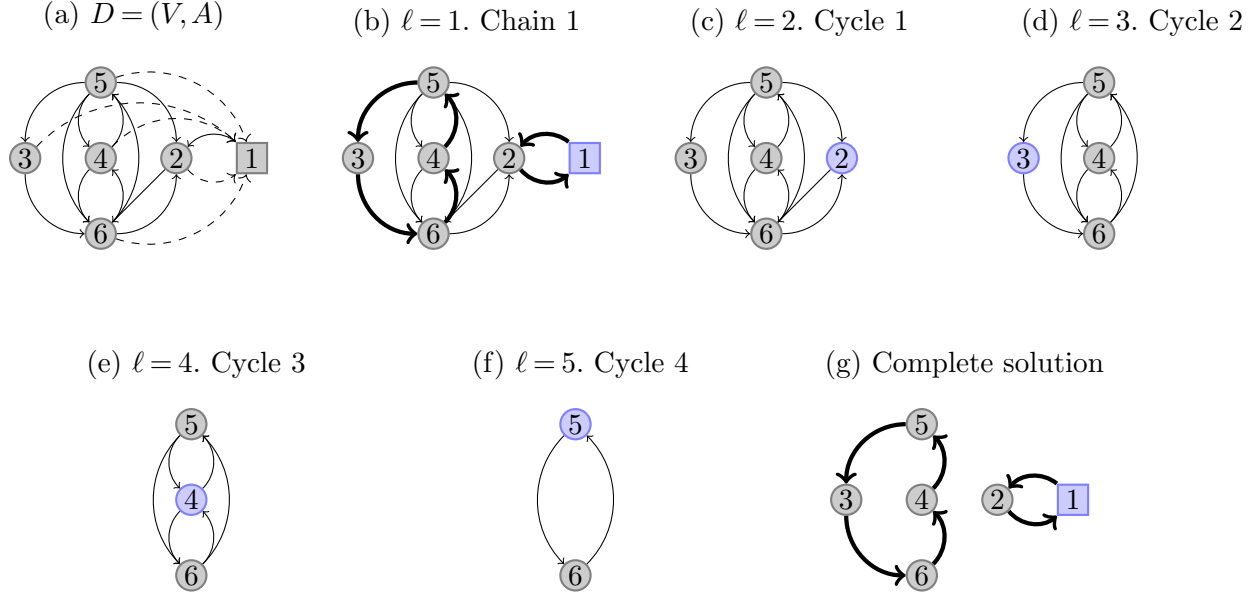


Figure 9 Counter example where (16) and (17) provide an infeasible solution. An altruistic donor is represented by a square and blue vertices correspond to the vertex with lowest index in the ℓ -th cycle or chain. Dashed arcs indicate compatibility of paired donors with a dummy patient associated to the altruistic donor, solid arcs indicate compatibilities among real donors and patients, and bold arcs represent the ones selected in a solution.

B.2. EEF: Extended Edge Formulation

Consider $\mathcal{P} + \mathcal{N}$ copies of the graph D , $D^\ell = (V^\ell, A^\ell)$, where V^ℓ is as defined in Section B.1 and $A^\ell = \{(i, j) \in \mathcal{A} \mid i, j \in V^\ell\}$ is the set of arcs in the ℓ -th copy. Recall that \mathcal{P} and \mathcal{N} is an upper bound on the number of cycles and chains in a feasible solution, respectively. In each copy $\ell \in \{1, \dots, |\mathcal{N}|\}$ chains are triggered by the ℓ -th NDD and at most L arcs can be selected. In each copy $\ell \in \{|\mathcal{N}| + 1, \dots, |\mathcal{N}| + |\mathcal{P}|\}$, all cycles include the vertex with lowest index in that copy (e.g., see Figure 9). Let x_{ij}^ℓ be an arc variable taking the value one if the arc $(i, j) \in A^\ell$ is selected in the

ℓ -th copy and zero, otherwise. Similarly to EAF, consider \mathcal{L} as the set of indices for which $V^\ell \neq \emptyset$.

Then, the extended edge formulation can be formulated as follows:

$$\max \sum_{\ell \in \mathcal{L}} \sum_{(i,j) \in A^\ell} w_{ij} x_{ij}^\ell \quad (17a)$$

$$\sum_{j:(j,i) \in A^\ell} x_{ji}^\ell = \sum_{j:(j,i) \in A^\ell} x_{ij}^\ell \quad \ell \in \mathcal{L}, i \in V^\ell \quad (17b)$$

$$\sum_{\ell \in \mathcal{L}} \sum_{j:(i,j) \in A^\ell} x_{ij}^\ell \leq 1 \quad i \in V \quad (17c)$$

$$\sum_{(i,j) \in A^\ell} x_{ij}^\ell \leq L \quad \ell \in \{1, \dots, |\mathcal{N}|\} \quad (17d)$$

$$\sum_{(i,j) \in A^\ell} x_{ij}^\ell \leq K \quad \ell \in \{|\mathcal{N}| + 1, \dots, |\mathcal{P}| + |\mathcal{N}|\} \quad (17e)$$

$$\sum_{j:(i,j) \in A^\ell} x_{ij}^\ell \leq \sum_{j:(\ell,j) \in A^\ell} x_{\ell j}^\ell \quad \ell \in \mathcal{L}, i \in V^\ell \quad (17f)$$

$$x_{ij}^\ell \in \{0, 1\} \quad \ell \in \mathcal{L}, (i, j) \in A^\ell \quad (17g)$$

Constraints (17b) assure that a patient in the ℓ -th graph copy receives a kidney if his or her paired donor donates one. Constraints (17c) allow every donor (paired or singleton) to donate at most one kidney in only one copy of the graph. Constraints (17d) and (17e) guarantee the maximum length allowed for chains and cycles in terms of arcs. Constraints (17f) assure that a copy is selected, only if the vertex with the lowest index is selected. Lastly, constraints (17g) define the nature of the decision variables.

The same counter example used for the EAF defined in Section B.1 applies to the EEF. For the example given in Figure (9), consider $K = 3$ and $L = 6$. Note that only the chain copy is selected, but due to the presence of subtours of length superior to the cycle size limit, both formulations can provide an infeasible solution. Therefore, infeasible-cycle-breaking constraints are required for every chain copy.

C. Proofs

In this section, we provide the proofs on the validity of IEEF and the complexity of finding a positive-price column via MDDs. For the sake of consistency, the numeration of the following propositions coincides with that used in the main body of the paper.

PROPOSITION 2. IEEF is a correct formulation of the matching problem in the KEP.

Proof. First, we need to show that a feasible matching to the KEP, $M(K, L)'$, corresponds to a feasible solution to IEEF whose objective function value equals the sum of the arc weights in $M(K, L)'$, which is

$$\sum_{(u,v) \in \mathcal{A}(M(K,L)')} w_{uv}.$$

Formally, let $M(K, L)' = \mathcal{C}'_K \cup \mathcal{C}'_L$ where $\mathcal{C}'_K \subseteq \mathcal{C}_K$ and $\mathcal{C}'_L \subseteq \mathcal{C}_L$. Since there are as many chain copies as NDDs and a single NDD per copy, for a chain $p = (v_1, \dots, v_\ell) \in \mathcal{C}'_L$, there exists a unique copy $i \in \bar{I}$ for which the i -th NDD, u_i , corresponds to v_1 . We then denote by $\bar{I}' \subseteq \bar{I}$ the set of chain copies corresponding to altruistic donors in $\mathcal{N} \cap \mathcal{V}(M(K, L)) \neq \emptyset$, which can be empty, i.e., there are no chains in a feasible solution. Thus, we define \bar{x}' as

$$\bar{x}'_{uv} = \begin{cases} 1 & \text{if } (u, v) \in \mathcal{A}(p) \\ 0 & \text{o.w.} \end{cases} \quad \forall i \in \bar{I}', p = (u_i, v_2, \dots, v_\ell) \in \mathcal{C}'_L$$

and

$$\bar{x}'_{uv} = 0 \quad \forall i \in \bar{I} \setminus \bar{I}'.$$

In the case of cycles, suppose $\mathcal{V}^* = \{v_1, \dots, v_{|\mathcal{V}^*|}\}$ is a K -limited FVS provided by Algorithm 1. Then, for a cycle $c = (v_1, \dots, v_k, v_1) \in \mathcal{C}'_K$ at least one of its vertices is also in \mathcal{V}^* by the definition of a K -limited FVS (see Section A.1). Let e be the smallest position in \mathcal{V}^* where a feedback vertex $v_e^* \in \mathcal{V}(c)$ is at, which coincides with the position of that copy in \hat{I} . Then, for the cycle $c \in \mathcal{C}'_K$ we define

$$\hat{x}'_{uv} = \begin{cases} 1 & \text{if } (u, v) \in \mathcal{A}(c) \\ 0 & \text{o.w.} \end{cases} \quad \forall (u, v) \in \hat{\mathcal{A}}^e.$$

We set the other components of \hat{x}' vector similarly. At (\hat{x}', \bar{x}') , constraints (10a) are satisfied since $M(K, L)'$ is feasible, i.e., every donor can donate at most once. This unitary flow satisfies flow-balance constraints in cycle copies (10b) and chain copies (10c). By the construction of (\hat{x}', \bar{x}') , we know that at most one cycle/chain is selected in each copy, and they are the same cycles and

chains of $M(K, L)'$. Thus, it is easy to see that the sum of arc variables for cycle (10d) and chain (10e) copies does not exceed K and L , respectively. Constraints (10f) and (10g) are also satisfied since the left-hand side can take one as its maximum value, by (10a), and only arcs from the chain and cycle copies whose critical vertices u_i and v_i^* appear in $M(K, L)'$ are selected while constructing (\hat{x}', \bar{x}') . Observe that constraints (10h) are applied to cycles present in chain copies. They are satisfied by \bar{x}' since only the set of arcs forming a chain is selected in \bar{x}' for copies in \bar{I}' , and no arc is selected from copies in $\bar{I} \setminus \bar{I}'$.

Therefore, (\hat{x}', \bar{x}') is a feasible solution to IEEF. Lastly, it is easy to see that its objective value equals

$$\sum_{i \in \hat{I}} \sum_{(u,v) \in \hat{\mathcal{A}}^i} w_{uv} \hat{x}_{uv}^{i'} + \sum_{i \in \bar{I}} \sum_{(u,v) \in \bar{\mathcal{A}}^i} w_{uv} \bar{x}_{uv}^{i'} = \sum_{(u,v) \in \mathcal{A}(M(K,L))} w_{uv},$$

Again, by construction, we need to show for the reverse direction that any feasible solution of IEEF corresponds to a feasible matching of the KEP, $M(K, L)^*$. Let (\hat{x}^*, \bar{x}^*) be a feasible solution of IEEF. Because IEEF can have symmetric solutions, a cycle $c \in \mathcal{C}_K$ can be selected in (a) the cycle copy corresponding to its associated feedback vertex as determined by Algorithm 1, (b) another cycle copy, or (c) a chain copy. However, constraints (10f) allow case (b) only when the feedback vertex of that copy is also selected. Similarly, constraints (10g) allow case (c) only when the NDD associated to a chain copy is also selected. A chain, on the other hand, can only be selected in a unique chain copy by construction of the chain copies. From (10a), we guarantee that the flow leaving every vertex is at most one across all copies, whether they are cycle or chain copies. Thus, an arc traversal in IEEF is vertex-disjoint.

To build feasible cycles from (\hat{x}^*, \bar{x}^*) to include in $M(K, L)^*$, we start by inspecting the arc flow leaving feedback vertices in their corresponding copies, i.e., $\sum_{v: (v_i^*, v) \in \hat{\mathcal{A}}^i} \hat{x}_{v_i^* v} = 1, i \in \hat{I}$. Constraints (10b) enforce flow preservation, i.e., if a vertex gives one unit of flow, it must also receive one. Thus, the arc traversal starting from v_i^* must be a cycle and it is also simple by (10a). Constraint (10d) enforces the number of selected arcs in a cycle copy to be at most K . Thus, under case (a), the arc traversal is guaranteed to be a feasible cycle $c \in \mathcal{C}_K$. If $|\mathcal{A}(c)| \leq K - 2$, then we evaluate case (b),

since a cycle can still arise. We proceed to inspect the outgoing flow of other feedback vertices also present in that copy. It is easy to see that due to constraints (10a), (10b) and (10d) the new arc traversal is also a simple cycle $\tilde{c} \in \mathcal{C}_K$, such that $|\mathcal{A}(\tilde{c})| \leq K - |\mathcal{A}(c)|$. Thus, there can be as many cycles inside a cycle copy as long as the total number of arcs selected does not exceed K . Under case (c), when an NDD is selected in a chain copy, a subtour may also be selected. By constraints (10a) and (10c) one can see that such subtours correspond to simple cycles. Nonetheless, their cardinality can exceed K when $L > K$. Constraints (10h) remove all $c \in \bar{\mathcal{C}}^i \setminus \mathcal{C}_K^i$, $i \in \bar{I}$, thus, guaranteeing that if a subtour is selected it corresponds to a feasible cycle.

To include chains in $M(K, L)^*$, constraints (10a), (10c) and (10e) guarantee the arc traversal in a chain copy to contain a feasible chain. Note that all the cycles and chains included in $M(K, L)^*$ are vertex-disjoint due to (10a). Lastly, the weight of each arc variable in IEEF has a one-to-one correspondence with a transplant weight in $M(K, L)^*$. Thus, the objective value of (\hat{x}^*, \bar{x}^*) corresponds to $\sum_{(u,v) \in \mathcal{A}(M(K,L)^*)} w_{uv}$, which completes the proof. \square

PROPOSITION 4. Given the reduced costs \hat{r}_c^i and \bar{r}_p^i expressed as an arc-separable function for all $(n_s, n_{s'}) \in \hat{\mathcal{A}}^i$ and $(n_s, n_{s'}) \in \bar{\mathcal{A}}^i$, a positive-price cycle, if one exists, can be found in time $\mathcal{O}(\sum_{i \in \hat{I}} \sum_{(n_s, n_{s'}) \in \hat{\mathcal{A}}^i} |\delta_-^i(n_s)|)$. Similarly, a positive-price chain can be found in $\mathcal{O}(\sum_{i \in \bar{I}} \sum_{(n_s, n_{s'}) \in \bar{\mathcal{A}}^i} |\delta_-^i(n_s)|)$.

Proof. For every arc $(n_s, n_{s'}) \in \hat{\mathcal{A}}^i$ and $(n_s, n_{s'}) \in \bar{\mathcal{A}}^i$, $|\delta_-^i((n_s, n_{s'}))|$ comparisons need to be performed to obtain $\hat{\eta}^i((n_s, n_{s'}))$ and $\bar{\eta}^i((n_s, n_{s'}))$, respectively in (2). Thus, for the i th MDD of a cycle copy, $\sum_{(n_s, n_{s'}) \in \hat{\mathcal{A}}^i} |\delta_-^i(n_s)|$ comparisons are required to compute $\hat{\eta}^i$, whereas for the i th MDD of a chain copy, there are the same number of comparisons plus $|\bar{\mathcal{A}}^i|$ comparisons of all arcs, in (3b), before obtaining $\bar{\eta}^i$. Since there are $|\hat{I}|$ cycle MDDs and $|\bar{I}|$ chain MDDs, it follows that the time complexity is as shown above. \square

PROPOSITION 5. The size of the input $\sum_{i \in \hat{I}} \sum_{(n_s, n_{s'}) \in \hat{\mathcal{A}}^i} |\delta_-^i(n_s)|$ grows as $|\hat{\mathcal{V}}^i|^{K+1}$ does.

Proof. Without loss of generality, assume \mathcal{D} is complete. As stated before, the layer of an arc $a : (n_s, n_{s'}) \in \hat{\mathcal{A}}^i$ is the layer to which its source node belongs, i.e., if node $n_{s'}$ is on layer k , then

$\ell(a) = k$. Moreover, let $\hat{\mathcal{A}}_k^i := \{a \in \hat{\mathcal{A}}^i \mid \ell(a) = k\}$ be the set of arcs that belong to layer k . By construction of the MDDs, \mathbf{r} has only one outgoing arc such that $\text{val}((\mathbf{r}, n_1)) = v_i^*$. In the second layer, \mathcal{L}_2 , the cardinality of $\hat{\mathcal{A}}_2^i$ can be up to $|\hat{\mathcal{V}}^i| - 1$ corresponding to the vertices $v \in \hat{\mathcal{V}}^i \setminus \{v_i^*\}$ that can be selected in the second position of a cycle. Note that since there can be the same number of 2-way cycles, an arc $a \in \hat{\mathcal{A}}_2^i$ has a sink node n such that $(n, \mathbf{t}) \in \hat{\mathcal{A}}^i$. If the length of a cycle is larger than two, then the cardinality of $\hat{\mathcal{A}}_3^i$ can be up to $|\hat{\mathcal{V}}^i| - 2$, representing the $|\hat{\mathcal{V}}^i| - 2$ vertices $v \in \hat{\mathcal{V}}^i \setminus \{v_i^*\}$ that can be selected in the third position of a cycle. The same process is repeated until in layer \mathcal{L}_K there are $|\hat{\mathcal{V}}^i| - (K - 1)$ vertices $v \in \hat{\mathcal{V}}^i$ to choose, and thus, $|\hat{\mathcal{V}}^i| - (K - 1)$ arcs $a \in \hat{\mathcal{A}}^i$ pointing to n . Thus, $|\hat{\mathcal{A}}^i|$ equals

$$\prod_{k=2}^K |\hat{\mathcal{V}}^i| - (k - 1) + \sum_{k=2}^{K-1} (|\hat{\mathcal{V}}^i| - (k - 1)) < |\hat{\mathcal{V}}^i|^{K-1} + K|\hat{\mathcal{V}}^i| \quad (18a)$$

The second sum on the left-hand side corresponds to the number of arcs at every layer whose sink node is n , thus, closing up cycles using fewer than K arcs. Therefore, under a worst-case scenario in which $|\delta_-^i(n_s)|$ and $|\hat{I}|$ tend to $|\hat{\mathcal{V}}^i|$, the complexity of finding a positive-price cycle becomes $\mathcal{O}(|\hat{\mathcal{V}}^i|^{K+1})$. \square

PROPOSITION 6. The size of the input $\sum_{i \in \bar{I}} \sum_{(n_s, n_{s'}) \in \hat{\mathcal{A}}^i} |\delta_-^i(n_s)|$ grows as $|\hat{\mathcal{V}}^i|^{L+2}$ does for bounded chains and as $|\hat{\mathcal{V}}^i|!$ when $L \rightarrow \infty$.

Proof. A similar reasoning to proposition 5 can be followed, except that a chain can be cut short if by visiting a new vertex $v \in \hat{\mathcal{V}}^i$ in a sequence of the state transition graph at least one PDP is present more than once, thereby violating the condition of being a simple path. We know that for a path to have L -many arcs, it is necessary to have a sequence with L PDPs, thus, $|\hat{\mathcal{A}}^i|$ tends to $|\hat{\mathcal{V}}^i|^L$ and $\sum_{i \in \bar{I}} \sum_{(n_s, n_{s'}) \in \hat{\mathcal{A}}^i} |\delta_-^i(n_s)| \approx |\hat{\mathcal{V}}^i|^{L+2}$. Therefore, for bounded chains, finding a positive-price chain can be done in time $\mathcal{O}(|\hat{\mathcal{V}}^i|^{L+2})$. The second part follows by the fact that after we visit ℓ vertices, there are still $|\hat{\mathcal{V}}^i| - \ell$ ways to choose the next one, until only one can be chosen, thus, the time to find a positive-price column when L is unbounded is exponential. \square

D. Additional Results

Columns by phase

Figure 10 depicts the type and number of columns found in each phase for individual runs across all the K - L combinations. The x -axis represents the total time (in minutes) to solve the pricing problem of a single run, i.e., an instance on a K - L setting, during the three phases. For every x -value there may be multiple y -points representing the number of columns found in a specific phase (sub phase) in thousands and whether they are cycle or chain columns. Therefore, for the same x -value, multiple y -values may correspond to the same instance, maybe on different settings, if the markers share the same size and color, regardless of the shape. For similar total pricing-problem times, markers may overlap. As an example, consider the time interval from 2min to 10min. In the cycle subplot there are big (purple) circle markers indicating that from 10k up to 30k cycle columns were found in Phase 1, as apposed to the chain subplot where no such markers appear. This means that this subset of instances correspond to $L = 0$. In another example, some instances with 2252 PDPs and 204 NDDs whose pricing time is 15.6min and have a green circle around 12k and 6k in the cycle and chain subplots, respectively, plus a triangle indicating one chain found through (LPH). Thus, the total number of columns of a run is the sum over the number of columns indicated by all markers in the y -axis with respect to the same x -value, provided that markers share color and size. In this particular case of 2048 PDPs and 204 NDDs there are 17,396 columns. Overall, most markers are circles, indicating that the majority of columns are found via MDDs across all runs, while Phase 2 and Phase 3 mostly certify that no more positive-price columns exist.

Effect of vertex-selection rules on BP_MDD

For instances in the set KEP_N0, Table 2 provides average values on the performance of BP_MDD in terms of the number of states (i.e., the number of nodes in MDDs) and the solution time when different selection rules are used in Algorithm 1. Selection rule Incr.Index corresponds to selecting every pair in the graph in increasing order of their index, as in (Constantino et al. 2013).

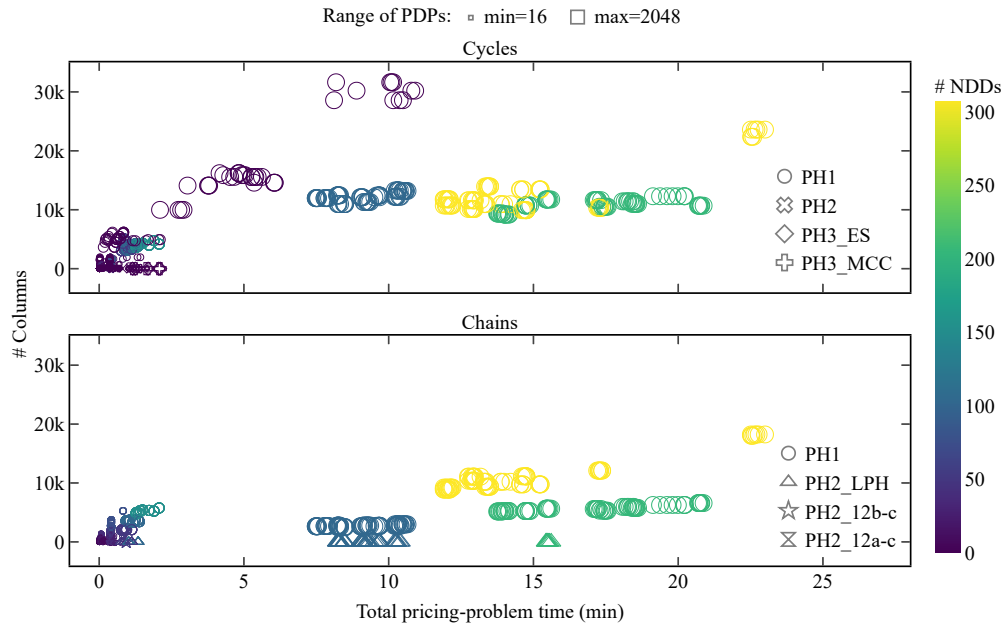


Figure 10 Classification of columns by run, phase (PH1, PH2, PH3) and type. Marker types indicate different (sub) phases of column generation. Marker sizes are correlated with the number of PDPs, while marker colors indicate the number of NDDs. ES stands for the Exhaustive Search in PH2.

The column K -FVS corresponds to finding the K -FVS with smallest cardinality through a MIP formulation. This formulation was given a time limit of 1hr. There is a hyphen if a feasible solution was not available after this time.

Table 2 Trade-off between performance and scalability when $K = 3$

Set	Average # States				Solution Time (s)			
	K -FVS	Incr.Index	Indegree	Total degree	K -FVS	Incr.Index	Indegree	Total degree
N16_A0	10.4	20.3	12.0	11.4	0.00	0.00	0.00	0.00
N32_A0	74.9	124.1	73.2	73.4	0.00	0.00	0.00	0.00
N64_A0	283.7	479.8	229.5	282.4	0.01	0.01	0.01	0.01
N128_A0	1,281.5	1,753.6	933.9	1,192.2	0.03	0.02	0.02	0.02
N256_A0	6,270.3	7,542.1	4,038.2	5,646.7	0.22	0.14	0.15	0.15
N512_A0	29,805.3	31,531.5	16,158.9	25,537.5	1.62	0.96	1.44	1.34
N1024_A0	-	129,608.1	65,816.1	112,277.8	-	8.35	22.84	42.40
N2048_A0	-	513,423.8	252,659.7	467,831.7	-	85.29	521.25	484.82

Even though, Incr.Index reports the smallest solution time on average, the number of states throughout all MDDs double those of the Indegree selection rule. This selection rule offers the best trade-off between scalability and computational performance.

Prioritization for instances in KEP_N

Table 3 shows the solution composition under the two prioritization schemes for a sample of the instance sets in KEP_N. Header names are defined as in Table 1 of the Results Section. It was worth noting that, except for 23 runs in the set N588_A76, all altruistic donors were used to trigger chains. For those runs, the percentage of used altruistic donors was 98.7%.

Table 3 Solution composition by execution modes

Set	K	L	Averages on CH mode			Average Ratio CH/CY		
			AvChainLen	nCyclesSol	AvCycleLen	AvChainLen	nCycleSol	AvCycleLen
N147_A19	3	3	2.97	17.22	2.81	1.50	0.71	1.02
N147_A19	3	4	2.99	17.00	2.83	1.51	0.71	1.02
N147_A19	3	5	3.00	17.11	2.79	1.55	0.71	1.00
N147_A19	3	6	3.06	16.50	2.83	1.58	0.68	1.02
N147_A19	4	3	3.00	17.21	2.81	1.49	0.71	1.03
N147_A19	4	4	3.00	17.00	2.83	1.52	0.71	1.02
N147_A19	4	5	3.00	17.12	2.79	1.55	0.71	1.00
N147_A19	4	6	3.00	16.55	2.83	1.58	0.68	1.02
N294_A38	3	3	3.00	30.63	2.84	1.76	0.63	1.02
N294_A38	3	4	3.00	30.43	2.85	1.67	0.64	1.02
N294_A38	3	5	3.00	30.57	2.84	1.58	0.67	1.01
N294_A38	3	6	3.00	30.70	2.83	1.61	0.66	1.01
N294_A38	4	3	3.00	30.67	2.84	1.74	0.63	1.02
N294_A38	4	4	3.00	30.44	2.85	1.68	0.64	1.03
N294_A38	4	5	3.00	30.52	2.84	1.58	0.67	1.01
N294_A38	4	6	3.00	30.71	2.83	1.60	0.66	1.02
N588_A76	3	3	3.00	61.30	2.93	1.54	0.69	1.03
N588_A76	3	4	3.00	61.30	2.93	1.56	0.68	1.03
N588_A76	3	5	3.00	61.30	2.93	1.36	0.75	1.04
N588_A76	3	6	3.00	61.30	2.93	1.41	0.73	1.03
N588_A76	4	3	3.00	61.30	2.93	1.53	0.69	1.03
N588_A76	4	4	3.00	61.30	2.93	1.50	0.70	1.03
N588_A76	4	5	3.00	61.30	2.93	1.36	0.75	1.04
N588_A76	4	6	3.00	61.30	2.93	1.41	0.73	1.03